PAPER

New quinazolone–sulfonate conjugates with an acetohydrazide linker as potential antimicrobial agents: design, synthesis and molecular docking simulations†

Asmaa F. Kassem,[ab] Sherif S. Ragab, [iD][c] Mohamed A. Omar,[b] Najla A. Altwaijry, [iD][d] Mohamed Abdelraof,[e] Ahmed Temirak,[b] Asmaa Saleh[d] and Aladdin M. Srour [iD] *[f]

A novel molecular design based on a quinazolinone scaffold was developed *via* the attachment of aryl alkanesulfonates to the quinazolinone core through a thioacetohydrazide azomethine linker, leading to a new series of quinazolinone–alkanesulfonates **5a–r**. The antimicrobial properties of the newly synthesized quinazolinone derivatives **5a–r** were investigated to examine their bactericidal and fungicidal activities against bacterial pathogens like *Bacillus subtilis*, *Staphylococcus aureus* (Gram-positive), *Pseudomonas aeruginosa*, *Klebsiella pneumonia*, *Sallmonella Typhimurium* (Gram-negative), in addition to *Candida albicans* (unicellular fungal). The tested compounds demonstrated reasonable bactericidal activities compared to standard drugs. Notably, derivatives **5g** and **5k** exhibited the greatest MIC values against *Candida albicans*, while **5g** was the best against *Staphylococcus aureus* with MIC of 11.3 ± 2.38 $\mu g\ mL^{-1}$, two-fold efficacy more than that was recorded with sulfadiazine. Furthermore, **5k** significantly prevented biofilm formation for all bacterial pathogens, with a percentage ratio reaching 63.9%, surpassing the standard drug Ciprofloxacin. Additionally, **5k** caused elevated lipid peroxidation (LPO) when added to the tested microbial pathogens. Confocal Laser Scanning Microscopy (CLSM) visualization revealed fewer live cells after treatment. Molecular docking studies showed that the quinazolinone derivatives bind strongly to the DNA gyrase enzyme, with the acid hydrazide core interacting effectively with key residues GLU50, ASN46, GLY77, and ASP136, consistent with their antimicrobial activity. Additionally, these compounds exhibited promising physicochemical properties, paving the way for discovering new antimicrobial drugs.

1. Introduction

Increasing multidrug-resistant (MDR) microorganisms have become one of the most crucial threats to healthcare in the current era.[1] The World Health Organization describes antimicrobial resistance as a natural phenomenon caused by bacteria that can no longer respond to treatments to which they were previously sensitive.[2,3] Despite recent advances in resistance mechanisms, drug-resistant microorganisms continue to pose a threat to our ability to heal common diseases and are becoming increasingly deadly.[4–6] In the past, antibiotic-resistant bacteria were rare and mainly associated with nosocomial infections, but today, they have become very common. Especially alarming is the pace at which multi- and pan-resistant bacteria spread around the globe and infect people with diseases that are not treatable with antibiotics or other antimicrobials.[2] Moreover, the coronavirus 2 pandemic (COVID-19)[7–9] also worsened the MDR issue as a result of the widespread exposure of patients to antibiotics.[9] The most common pathogens include *Enterococcus faecalis*, *Klebsiella pneumonia*, *Staphylococcus* species involving *Staphylococcus aureus* and *Staphylococcus epidermidis*, in addition to the predominant pathogens involving *Enterobacter*, *Pseudomonas aeruginosa,* and *Acinetobacter baumannii*.[10–12] The new versions of antibiotics that are currently approved have a similar structure close to the previous drugs, thus they are expected to confront the same

[a]Department of Chemistry, College of Science and Humanities in Al-Kharj, Prince Sattam Bin Abdulaziz University, Al-Kharj, 11942, Saudi Arabia

[b]Chemistry of Natural and Microbial Products Department, Pharmaceutical and Drug Industries Research Institute, National Research Centre, Dokki, Giza, 12622, Egypt

[c]Photochemistry Department, Chemical Industries Research Institute, National Research Centre (NRC), 33 El-Behouth St., P.O. 12622, Dokki, Giza, Egypt

[d]Department of Pharmaceutical Sciences, College of Pharmacy, Princess Nourah Bint Abdulrahman University, P.O. Box 84428, Riyadh 11671, Saudi Arabia

[e]Microbial Chemistry Department, National Research Centre, Biotechnology Research Institute, Giza, Egypt

[f]Department of Therapeutic Chemistry, Pharmaceutical and Drug Industries Research Institute, National Research Centre, Dokki, Giza, 12622, Egypt. E-mail: aladdinsrour@gmail.com

† Electronic supplementary information (ESI) available. See DOI: https://doi.org/10.1039/d4ra07563c

pathways of bacterial resistance.[13,14] As a result, there is a pressing requirement to create and develop new antibiotics using innovative methods to effectively combat multidrug-resistant organisms.[15] In their continuous quest to find lead compounds capable of combating bacterial resistance, researchers have identified a range of compounds, and the potential to develop antimicrobial agents is ongoing in all directions. In this context, molecular hybridization emerged as a promising methodology effectively utilized to exert synergistic effects against MDR diseases by encompassing multiple pharmacophores in a single molecule.[16,17]
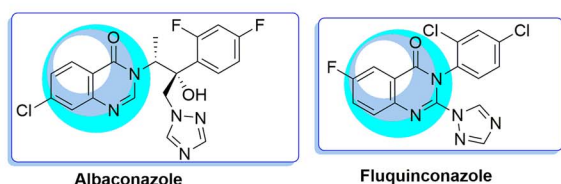
Quinazolinones, a bicyclic system of pyrimidinone and benzene rings, dominate the field of medicinal chemistry and represent the winning horse in drug discovery.[18,19] In terms of synthetic as well as biological implications, quinazolinones are quite intriguing and could provide effective treatment options for public health issues. Although quinazolinones were reported for a long time, their synthesis and applications in diverse fields are still topical and have captivated organic and medicinal chemists for decades.[20] Numerous quinazolinone-based drugs have been approved and spread in the markets such as idelalisib, arofuto, afloqualone, mecloqualone, ispinesib, balaglitazone, nolatrexed, raltiltrexed, halofuginone.[21] Albaconazole[22] and Fluquinconazole[23] represent the more interesting quinazolinone-based drugs in our study where they are widely used as antimicrobial agents (Fig. 1). Recently, gained momentum has been directed to the utilization of

quinazolinone as a core for the formulation of new antibacterial drug leads.[24]

On the other hand, hydrazide–hydrazone derivatives, hydrazide molecules with azomethine functionality (–CONHN=CH–), were shown to exhibit prominent pharmacological and biological properties, such as antimicrobial, anti-inflammatory, analgesic, anticancer, anticonvulsant, antiviral, antiprotozoal, antiplatelet, antimalarial, antimycobacterial, vasodilator, and antischistosomiasis activities.[25,26] Various studies reported that hydrazide–hydrazone functionalities in biological systems can easily undergo hydrolysis, which can be advantageous in treating a variety of life-threatening diseases.[27,28] The antimicrobial activity of this class of compounds represents the most frequently encountered in scientific literature among the biological properties.[27] Indeed, nitrofurazone, furazolidone, and nitrofurantoin (Fig. 1) are widely used antimicrobial drugs and are considered typical examples of chemotherapeutic agents containing hydrazide–hydrazone moiety.[29]

Sulfonates have found widespread use in medical research and have significant pharmacological applications. The distinctive physicochemical properties of sulfonate-based compounds support their affinity for lipid phases causing a facile penetration through cell membranes to interact with the target sites.[30] Fenson, Chlorfenson, and Genite are aryl sulfonates that have long been marketed as insecticides,[31,32] while busulfan is an alkyl sulfonate drug that was approved as
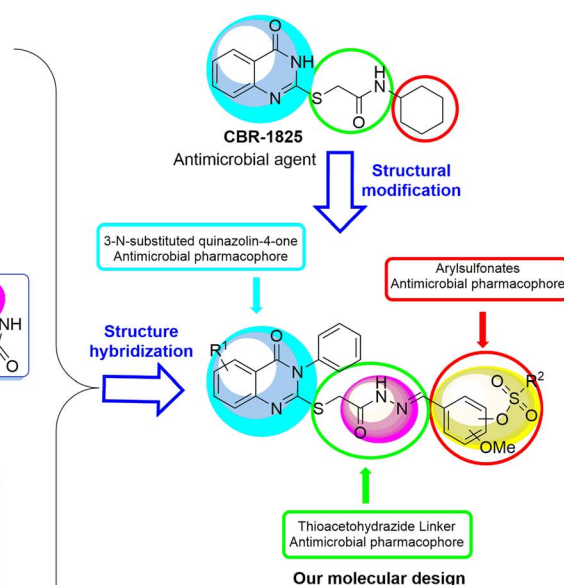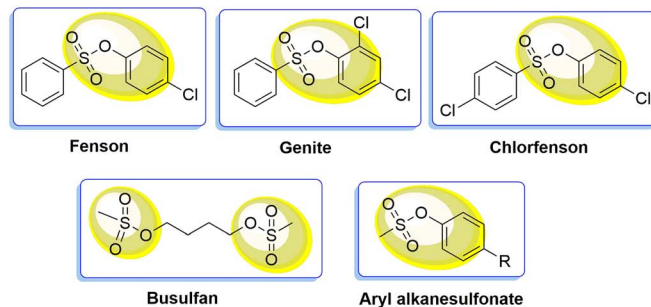

Fig. 1 Marketed drugs containing quinazolinone, hydrazide–hydrazone, or sulfonate motifs along with our molecular design.

a chemotherapy for the treatment of chronic myeloid leukemia (CML)[33] (Fig. 1). Aryl alkanesulfonates are a class of sulfonate-containing compounds of both alkyl and aryl substituents and have been screened as antifungal[34] anticancer,[35] acaricidal agents,[24] in addition to their use as inhibitors of carbonic anhydrase.[36] Using these results in conjunction with our previous research on pyrimidine antibacterial agents.[1] Our efforts are focused on developing novel molecular designs to get new quinazolinone-based scaffolds with anticipated antimicrobial activity. To achieve this, 2-((4-oxo-3,4-dihydroquinazolin-2-yl)thio)acetohydrazide **3** has been employed as a promising precursor for synthesizing new antimicrobial candidates. The design of this new series incorporates quinazolinone and sulfonate moieties, strategically positioned to bind with ARG136 and ARG76, respectively. Furthermore, the amide NH group of the acetohydrazide linker is designed to form hydrogen bonds with GLY77. This approach is compared to the known inhibitor 4-(4-bromo-1*H*-pyrazol-1-yl)-6-[(ethylcarbamoyl)amino]-*N*-(pyridin-3-yl)pyridine-3-carboxamide (CWW), to improve binding affinity and antimicrobial efficacy,[37,38] Fig. 1. The antimicrobial properties of the newly synthesized quinazolinone acetohydrazide sulfonates derivatives were investigated to examine their bactericidal and fungicidal activities against some clinical microbial pathogens.

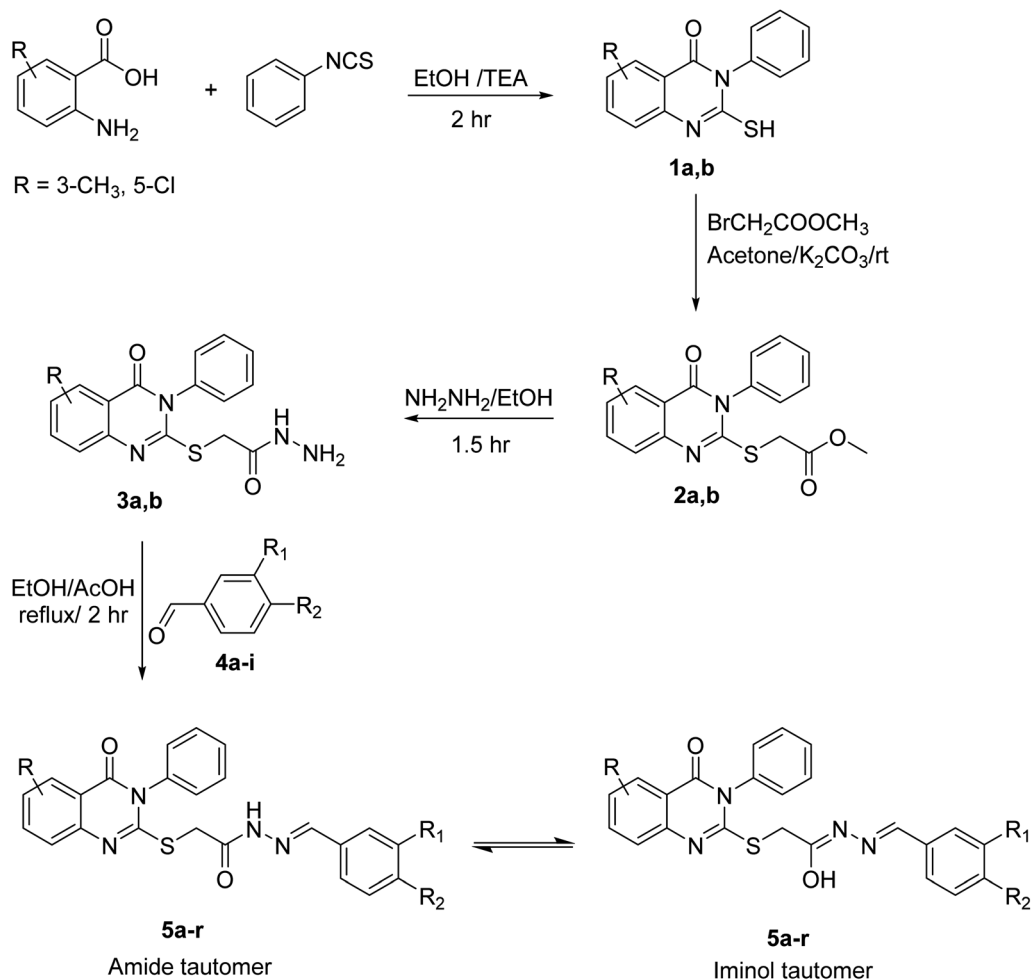## 2. Results and discussion

2.1. Chemistry

Our molecular design involves 2-((4-oxo-3,4-dihydroquinazolin-2-yl)thio)acetohydrazide **3** as a promising precursor for synthesizing new quinazolinone candidates. The latter conger was installed *via* attachment of aryl alkanesulfonates to the quinazolinone core *via* thioacetohydrazide azomethine linker, leading to a new series of quinazolinone-alkanesulfonates **5a–r**. The synthetic route toward this series was depicted in Scheme 1. Starting with the reaction of 2-amino-3-methylbenzoic acid or 2-amino-5-chlorobenzoic acid with phenyl isocyanate in ethanol in the presence of Et₃N yielded the corresponding 2-mercapto-3-phenylquinazolin-4(3*H*)-ones **1a,b**. Esterification of **1a,b** was then carried out using methyl bromoacetate to afford the corresponding esters **2a,b** which were then converted to the corresponding acetohydrazide analogs after heating under reflux in ethanol with hydrazine hydrate to give **3a,b**. Derivatives **3a,b** were the precursors for the final quinazoline-alkanesulfonate targets **5a–r** when heated in ethanol under reflux with various *para*-substituted aromatic aldehydes (bearing different alkane sulfonate moieties namely: methane, ethane or propane sulfonate moieties) **4a–i**. IR, ¹H & ¹³C-NMR, and elemental analyses have been exploited to reveal the chemical structure of the newly synthesized conjugates **5a–r**. Specifically, the IR spectra of **5a–r** revealed a strong stretching band around 3170 cm⁻¹ indicating the NH group, while the characteristic absorption bands of C=O and C=N appeared at 1669–1683 cm⁻¹ and 1618–1636 cm⁻¹, respectively. Moreover, the SO₂ band was observed between 1340 and 1388 cm⁻¹. The ¹H NMR spectra of **5a–r** confirmed the existence of alkanesulfonate moieties where they appeared within the upfield region as singlet signals,

triplet–quartet signals, or triplet–sextet–triplet signals for methyl, ethyl, or propyl chains, respectively. Furthermore, the methylene protons were exhibited as singlets at $\delta_H = 4.46$–4.51 ppm. Furthermore, ¹H NMR spectra of **5a–r** also showed two singlet signals in the range of $\delta_H = 3.88$–4.00 ppm and $\delta_H = 4.00$–4.51 ppm with the integration of 2H each corresponding to SCH₂C=O protons that validate the presence of iminol and amide tautomers, respectively. The existence of such tautomerism was also supported by the presence of two singlet signals with total integration of 1H due to the azomethine protons (HC=N) of both tautomers within the ranges of $\delta_H = 7.98$–8.06 and $\delta_H = 8.14$–8.28 ppm, and two peaks with only 1H integration appeared in the ranges $\delta_H = 11.66$–11.80 ppm and $\delta_H = 11.70$–11.83 ppm, due to OH proton in case of iminol and NH proton in amide tautomer, respectively. On the other hand, the characteristic peaks that represent the carbons of alkanesulfonate groups were depicted at the aliphatic zone of the ¹³C NMR spectra in the range of $\delta_C = 8.00$–52.46 ppm, while the peaks observed between $\delta_C = 34.26$ ppm and $\delta_C = 35.01$ ppm assumed to be for the methylene carbons. The characteristic azomethine carbons (HC=N) appeared between $\delta_C = 145.52$ ppm and $\delta_C = 145.93$ ppm, whereas the carbonyl carbon of the acetohydrazide moiety was detected in the range of $\delta_C = 167.32$–168.75 ppm. Spectral charts of the new chemical entities **5a–r** are included in in ESI file (Fig. S2–S37),† The purity of the final compounds was determined by LC-MS using the area percentage method on the UV trace recorded at a wavelength of 254 nm and found to be >95%, representative charts of HPLC purity are displayed in ESI file (Fig. S38–S40).†

2.2. Antimicrobial activity

The newly synthesized molecules **5a–r** have been evaluated for their *in vitro* antibacterial properties, on *Bacillus subtilis*, *Staphylococcus aureus* (Gram-positive), *Pseudomonas aeruginosa*, *Klebsiella pneumonia*, *Salmonella typhimurium* (Gram-negative), and *Candida albicans* (unicellular fungal) (Fig. S1†). The preliminary results displayed in Table S1† revealed that derivatives **5a–c,e–h,k,l,n,p** were found to be potent inhibitors against some of the tested pathogens, while not able to inhibit the proliferation of other microbial strains. The high resistance of some pathogens reflects their virulence and rapid proliferation ability even upon being treated with some standard antibiotics such as Cephradine. Accordingly, most of the tested molecules failed to show any activity on MDR pathogens such as *Staphylococcus aureus* MRSA, *Salmonella typhimurium*, and *Pseudomonas aeruginosa*, which the inhibitory activity ranged from inactive to weak (not exceeding 3 mm of the inhibition zone). Derivatives **5f**, **5g**, and **5k** demonstrated promising inhibitory activity against all MDR pathogens, particularly the methyl-substituted quinazoline's phenyl derivatives **5f** and **5g** rather than the corresponding chloro analog **5k**. Moreover, compounds **5a**, **5f**, **5g** and **5h** displayed plausible inhibitory effects as anti-candida, which could represent good antifungal candidates among the tested series. On the other hand, no promising inhibition response was obtained by the tested series **5a–r** towards the MDR; *Salmonella typhimurium*, and

Scheme 1 The synthetic route toward quinazolone–sulfonate conjugates with their tautomers **5a–r**.

4a; $R_1 = H$, $R_2 = OSO_2CH_3$
4b; $R_1 = H$, $R_2 = OSO_2CH_2CH_3$
4c; $R_1 = H$, $R_2 = OSO_2CH_2CH_2CH_3$
4d; $R_1 = OCH_3$, $R_2 = OSO_2CH_3$
4e; $R_1 = OCH_3$, $R_2 = OSO_2CH_2CH_3$
4f; $R_1 = OCH_3$, $R_2 = OSO_2CH_2CH_2CH_3$
4g; $R_1 = OSO_2CH_3$, $R_2 = OCH_3$
4h; $R_1 = OSO_2CH_2CH_3$, $R_2 = OCH_3$
4i; $R_1 = OSO_2CH_2CH_2CH_3$, $R_2 = OCH_3$

5a; $R = 3\text{-}CH_3$, $R_1 = H$, $R_2 = OSO_2CH_3$
5b; $R = 3\text{-}CH_3$, $R_1 = H$, $R_2 = OSO_2CH_2CH_3$
5c; $R = 3\text{-}CH_3$, $R_1 = H$, $R_2 = OSO_2CH_2CH_2CH_3$
5d; $R = 3\text{-}CH_3$, $R_1 = OCH_3$, $R_2 = OSO_2CH_3$
5e; $R = 3\text{-}CH_3$, $R_1 = OCH_3$, $R_2 = OSO_2CH_2CH_3$
5f; $R = 3\text{-}CH_3$, $R_1 = OCH_3$, $R_2 = OSO_2CH_2CH_2CH_3$
5g; $R = 3\text{-}CH_3$, $R_1 = OSO_2CH_3$, $R_2 = OCH_3$
5h; $R = 3\text{-}CH_3$, $R_1 = OSO_2CH_2CH_3$, $R_2 = OCH_3$
5i; $R = 3\text{-}CH_3$, $R_1 = OSO_2CH_2CH_2CH_3$, $R_2 = OCH_3$
5j; $R = 5\text{-}Cl$, $R_1 = H$, $R_2 = OSO_2CH_3$
5k; $R = 5\text{-}Cl$, $R_1 = H$, $R_2 = OSO_2CH_2CH_3$
5l; $R = 5\text{-}Cl$, $R_1 = H$, $R_2 = OSO_2CH_2CH_2CH_3$
5m; $R = 5\text{-}Cl$, $R_1 = OCH_3$, $R_2 = OSO_2CH_3$
5n; $R = 5\text{-}Cl$, $R_1 = OCH_3$, $R_2 = OSO_2CH_2CH_3$
5o; $R = 5\text{-}Cl$, $R_1 = OCH_3$, $R_2 = OSO_2CH_2CH_2CH_3$
5p; $R = 5\text{-}Cl$, $R_1 = OSO_2CH_3$, $R_2 = OCH_3$
5q; $R = 5\text{-}Cl$, $R_1 = OSO_2CH_2CH_3$, $R_2 = OCH_3$
5r; $R = 5\text{-}Cl$, $R_1 = OSO_2CH_2CH_2CH_3$, $R_2 = OCH_3$

Pseudomonas aeruginosa except derivatives **5a**, **5f**, and **5g**. *Bacillus subtilis* also exhibited a potent resistance towards most of the tested molecules, except for derivatives **5a**, **5f**, and **5g** (methyl-substituted quinazoline's phenyl derivatives) and **5k**, **5n**, and **5o** (chloro-substituted quinazoline's phenyl derivatives). Nonetheless, a reasonable inhibitory activity towards

Table 1 MIC of the most potent synthesized derivatives **5f**, **5g** and **5k**[a]

| | (MIC, μg mL^{-1}) | | | | | |
| | Unicellular fungal | Gram-positive bacteria | | Gram-negative bacteria | | |
Compd. ID	*Candida albicans*	*Bacillus subtilis*	*Staphylococcus aureus*	*Salmonella typhimurium*	*Klebsiella pneumonia*	*Pseudomonas aeruginosa*
5f	48 ± 4.18	23 ± 2.21	50 ± 0.88	49 ± 1.28	22 ± 4.72	45 ± 6.11
5g	9 ± 3.17	48 ± 2.25	11.3 ± 2.38	95 ± 2.05	99 ± 5.02	96 ± 4.83
5k	10 ± 2.55	49 ± 2.77	52 ± 0.28	21 ± 5.35	44 ± 1.88	97 ± 3.88
Sulfadiazine	72 ± 3.44	46 ± 4.18	24 ± 3.92	94 ± 2.29	47 ± 3.18	70 ± 4.99

[a] *Bacillus subtilis*, *Staphylococcus aureus* (Gram-positive), *Pseudomonas aaerginousea*, *Klebsiella pneumonia*, *Sallmonella Typhemerium* (Gram-negative), and *Candida albicans* (unicellular fungal) Dimethyl sulfoxide (DMSO) was used as a negative control.

Klebsiella pneumonia was noticed for all derivatives except for derivatives **5e** and **5n**, Table S1.† Consequently, the minimum inhibition concentration (MIC) for the most potent molecules **5f**, **5g** and **5k** has been determined to provide the lowest microbial growth following the standard procedure.[39] As shown in Table 2, brilliant inhibitory activity at lower concentrations has been recorded by derivatives **5g** and **5k** against *Candida albicans* (9 ± 3.17 and 10 ± 2.55 μg mL^{-1}, respectively) which exceeds by 7-fold the activity of the standard antifungal agent Sulfadiazine (72 ± 3.44 μg mL^{-1}). Likewise, derivative **5g** also exhibited a potent inhibitory effect towards *Staphylococcus aureus* at 11.3 ± 2.38 μg mL^{-1}, reflecting a 2-fold efficacy more than the standard antibacterial agent Sulfadiazine (24 ± 3.92 μg mL^{-1}) Table 1. Furthermore, compound **5f** provided a significant MIC value against both Gram-positive pathogens and Gram-negative bacteria, the MIC values of compound **5f** against *Bacillus subtilis*, *Klebsiella pneumonia*, *Salmonella typhimurium* and *Pseudomonas aeruginosa* were exceeding to that calculated for the corresponding reference antibiotic agents.

2.3. Antibiofilm of the targeted molecules

Inhibiting biofilm formation is one of the most effective ways to eradicate bacterial proliferation under stress conditions. Most bacterial pathogens protect themselves from stress by forming biofilms. Furthermore, biofilm formation is an important mechanism that makes bacterial pathogens more resistant to many traditional antibiotics. Biofilms primarily form in hostile environments surrounding the bacterial medium. This biofilm mechanism is commonly associated with the high resistance of bacterial pathogens and prevents the complete inhibition of bacterial cells when treated with antibacterial agents. Therefore, biofilm inhibitors are considered highly important compounds for enhancing the efficacy of antibacterial agents. Consequently, discovering new molecules that prevent or inhibit biofilm formation by bacterial pathogens has become increasingly desirable.

To investigate the biofilm inhibitory activity of our potent molecules, we utilized the crystal violet method to assess their effectiveness in eradicating established biofilms of bacterial pathogens. As indicated in Table 2, derivative **5k** demonstrated a significant ability to prevent biofilm formation by bacterial pathogens, particularly against *Bacillus subtilis* and *Salmonella typhimurium*. Similarly, compound **5f** showed considerable biofilm inhibition of *Staphylococcus aureus*, exhibiting antibiofilm activity that exceeded that of the standard drug, Ciprofloxacin. A slightly lower activity was observed for compound **5g**, particularly against Gram-negative bacteria. However, despite the promising activity of **5k**, a remarkably high resistance to biofilm formation was detected in *Pseudomonas aeruginosa*.

2.4. Effect of the targeted molecules on the bacterial lipid peroxidation (LPO)

A difficult penetration of the bacterial cytoplasmic membrane is considered an important tool to evaluate the inhibition by the tested treatments, which demonstrates the abilities of these

Table 2 Antibiofilm activity of the most potent synthesized derivatives **5f**, **5g** and **5k**[a]

| | Biofilm inhibition (%) | | | | |
| | Gram-positive bacteria | | Gram-negative bacteria | | |
Sample no.	*Bacillus subtilis*	*Staphylococcus aureus*	*Klebsiella pneumonia*	*Salmonella typhimurium*	*Pseudomonas aeruginosa*
5f	56.4 ± 3.12	45.1 ± 1.62	59.6 ± 2.22	37.4 ± 1.82	34.8 ± 4.07
5g	45.1 ± 2.72	34.7 ± 4.02	32.8 ± 1.92	33.9 ± 2.94	20.1 ± 2.32
5k	63.7 ± 0.92	42.9 ± 2.62	53.1 ± 2.12	61.9 ± 1.72	38.7 ± 3.66
Ciprofloxacin	49.2 ± 1.16	30.9 ± 4.52	40.8 ± 3.88	58.3 ± 4.02	45.2 ± 1.18

[a] Dimethyl sulfoxide (DMSO) was used as a negative control.

Table 3 Lipid peroxidation efficiency of the potent molecules **5f**, **5g** and **5k** against bacterial pathogens

	Lipid peroxidation efficiency (%)				
	Gram-positive bacteria		Gram-negative bacteria		
Sample no.	*Bacillus subtilis*	*Staphylococcus aureus*	*Klebsiella pneumonia*	*Salmonella typhimurium*	*Pseudomonas aeruginosa*
5f	212.5 ± 5.52	151.2 ± 1.92	230.4 ± 2.12	273.1 ± 4.33	140.4 ± 5.02
5g	219.7 ± 2.71	118.4 ± 2.26	285.2 ± 1.44	210.4 ± 4.66	175.2 ± 3.29
5k	377.6 ± 3.44	202.2 ± 2.17	295.2 ± 1.89	278.3 ± 5.07	181.3 ± 6.06
Ciprofloxacin	417.7 ± 2.83	319.8 ± 3.26	327.4 ± 4.42	294.8 ± 1.99	346.3 ± 2.62

treatments to make differences in the inhibition process, oxidative stress on the bacterial cell wall usually triggers oxidation of the cell wall fatty acid content leading to easily penetration of the tested compound inside the bacterial cell. The level of the obtained lipid peroxidation refers to the success of the treatment in overcoming the lysis cell wall problem. Therefore, an LPO test took place to evaluate the oxidation potential of bacterial cell membrane fatty acids by targeted molecules. Accordingly, treatments of each tested bacterial strain using the potent molecules at the MIC level were investigated (Table 3).

In this respect, there were significant variations in lipid peroxidation activity between the targeted molecules. There is a significant LP activity of **5k** when added to *Bacillus subtilis*, *Salmonella typhimurium*, and *Klebsiella pneumonia*. The LP result for these pathogens proved to be somewhat close to that obtained by the standard antibacterial agents. Moreover, **5k** also caused an elevated LP in the case of *Staphylococcus aureus* ($202.2 \pm 2.17\%$), however a lower LP activity in the case of *Pseudomonas aeruginosa* was indicated when compared to the standard drug. Overall, the positive response of the bacterial pathogens, *Bacillus subtilis*, *Salmonella typhimurium*, and *Klebsiella pneumonia* to the LP activity was demonstrated for the tested compounds. In addition, the strong resistance of both *Pseudomonas aeruginosa* and *Staphylococcus aureus* toward the LP activity reflected their virulence.

2.5. Confocal laser scanning microscope

The different observations of the potent compounds (*i.e.* **5f** and **5k**) effectiveness on the microbial pathogens were detected by a Confocal Laser Scanning Microscope (CLSM). As shown in (Fig. 2), a clear effect of the potent molecules on the biofilm and morphological observations was indicated. Since, a high concentration of the dead cells (red color) was found to be more prevalent, while a lower number of live cells were observed after treatment. The activity of the potent molecules was sharply indicated in the live cell concentration, particularly in the case of *Bacillus subtilis*, *Salmonella typhimurium* and *Klebsiella pneumonia.*

The right set of panels displayed the strains were allowed to form on glass-bottomed chambers for 24 h with acridine dye before being treated with the indicated antimicrobials (green color). The medium set of panels displayed the concentration of dead cells after treatment with target molecules (red color). The left set of panels displayed the negative control (black), untreated cells (off-white), live cells (green) and dead cells (red).

2.6. Cytotoxic properties

The safety of the powerful antimicrobial compounds, **5f**, **5g**, and **5k**, on the BJ1 cell line was assessed using the MTT assay. Notably, the study's findings showed that these substances did not cause cytotoxicity to the tested cells; however, their safety profile should be assumed after the necessary *in vivo* investigations are completed (Table S3†).

2.7. Docking studies on DNA gyrase enzyme

DNA gyrase is an essential enzyme in bacteria, responsible for introducing negative supercoils into DNA, which is crucial for DNA replication, transcription, and overall genomic stability. This enzyme inhibition is particularly effective against a broad spectrum of Gram-negative and some Gram-positive bacteria, making it a prime target for antibacterial agents. In our study, we investigated the antimicrobial properties of newly synthesized quinazolinone derivatives **5a–r** against various Gram-negative bacteria (*Klebsiella pneumoniae*, *Salmonella typhimurium*, *Pseudomonas aeruginosa*) and Gram-positive bacteria (*Bacillus subtilis*, *Staphylococcus aureus*). We performed detailed molecular docking studies of these compounds with the DNA gyrase enzyme to elucidate the molecular basis of their antimicrobial effects. The *E. coli* Gyrase B enzyme in complex with the known inhibitor 4-(4-bromo-1*H*-pyrazol-1-yl)-6-[(ethylcarbamoyl)amino]-*N*-(pyridin-3-yl)pyridine-3-carboxamide (CWW) was obtained from the Protein Data Bank (PDB code: 6F86).[40,41] Biovia Discovery Studio was employed to prepare the DNA gyrase enzyme for docking studies.[41,42] Extraneous chains and water molecules were removed, retaining HOH616 due to its role in forming a hydrogen-bonding network with the pyridyl ring's nitrogen atom and the amino acid residues ASP73, THR165, and GLY77.[41] Polar hydrogens were added. Partial charges were adjusted to accurately represent electrostatic interactions between the ligand and the binding site, thereby influencing the predicted binding pose and interaction quality. Docking simulations were then performed using Autodock 4 to predict the interactions of the quinazolinone derivatives with the DNA gyrase enzyme.[43] Autodock 4 was then used to predict the interactions between the synthesized quinazolinone derivatives (**5a–r**) and the DNA gyrase enzyme. This allowed us to calculate binding energies and visualize ligand positioning within the enzyme's active site, providing deeper insights into the binding mechanisms. Moreover, to validate our docking procedure, we re-docked the co-crystallized native ligand (CWW) into the DNA gyrase active site. The resulting pose
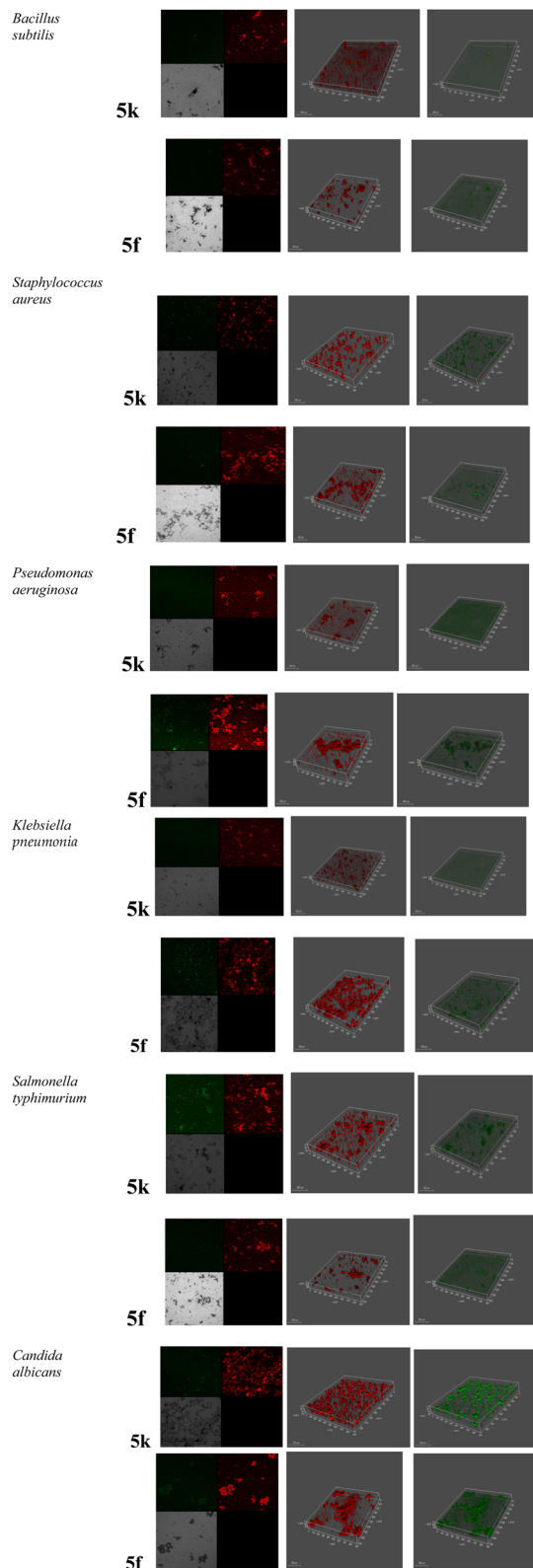
Fig. 2 The effect of the promising compounds **5f** and **5k** on the proliferation of the microbial pathogens *via* Confocal Laser Scanning Microscope (CLSM).

closely matched the original binding conformation, with binding affinities of -11.72 kcal mol^{-1}. It also demonstrated a RMSD (root mean square deviation) of 0.65. This close

alignment indicates a successful reproduction of the native ligand's binding mode, thus confirming the validity of our docking protocol, Table S3.†

Detailed interaction analysis revealed that the terminal pyridyl moiety of CWW forms a hydrogen bond with ARG136 and engages in hydrophobic interactions with the ARG76 residue. The amide NH group exhibits hydrogen bonding with the GLY77 residue (Fig. 3). The pyridyl core of CWW is stabilized in the active site by a direct hydrogen bond with THR165 and an additional water-mediated hydrogen bond involving HOH616. The urea side chain also forms significant hydrogen bonds with ASP73 and ASN46. Additionally, the native ligand participates in several hydrophobic interactions (van der Waals, alkyl, and carbon–hydrogen bonds) with key residues such as VAL167, ALA47, VAL43, ILE78, ILE94, and PRO79 (Fig. 3). Molecular docking studies were meticulously conducted to investigate the interactions of quinazolinone derivatives **5f**, **5g**, and **5k** within the active site of the DNA gyrase enzyme. These studies aimed to understand how these compounds could potentially inhibit DNA gyrase, providing insights into their antimicrobial properties. In general, the sulfonate group in the quinazolinone derivatives was found to engage in hydrogen bonding, similar to the carbonyl group of the urea side chain in the native ligand, interacting with several amino acids such as ASN43, VAL120, SER121, ILE78, and ARG136 (Fig. 3–6). This indicates that the sulfonate group may significantly stabilize the compounds within the enzyme active site.

Moreover, the acid hydrazide core of the quinazolinone derivative exhibited similar binding interactions to the amide linker of the native ligand. This core formed interactions with residues GLU50, ASN46, GLY77, and ASP136, suggesting that the acid hydrazide core is crucial for the binding affinity and proper positioning of the derivatives within the active site. The carbonyl group in the acid hydrazide core of compound **5f** exhibited a notable hydrogen bonding interaction with the water molecule HOH616 as depicted in Fig. 4. This interaction is similar to that exhibited by the core pyridyl ring in the native ligand, as illustrated in Fig. 3.

Besides, the nitrogen atom of the quinazolinone moiety demonstrated a binding pattern analogous to the nitrogen of the terminal pyridyl moiety in the native ligand, particularly with the ASP136 residue. This interaction was notably observed with compound **5k**, highlighting the importance of this moiety in the binding process (Fig. 3 and 6). Comparing the molecular interactions of our compounds with the native ligand showed that the sulfonyl group increased the binding interactions with several H-bonds. Also, we noticed that changing the position of the sulfonyl group from the *m*- to the *p*- position of the terminal phenyl ring did not affect the binding interactions. Also, we noticed that the ester group near the sulfonyl group increased the binding interactions of the quinazolinone derivatives as observed in compounds **5f** and **5g**, which could be attributed to the presence of several H-bond acceptor groups and their tendency to establish several H-bonding within the DNA gyrase binding pocket or maybe also some intramolecular H-bonds. Finally, we think his comprehensive analysis of the molecular interactions highlights the critical binding features that
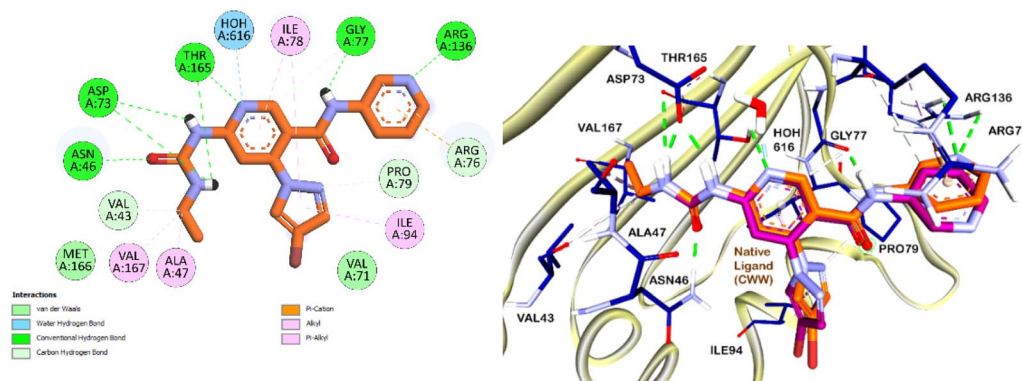
Fig. 3 (A) Superimposition of the native co-crystallized ligand CWW and the docked ligand within the DNA gyrase enzyme's binding site (PDB ID: 6F86). The native ligand's carbon atoms are depicted in violet, while the docked ligand's carbon atoms are shown in orange. (B) 2D interaction diagram of the docked CWW with the DNA gyrase enzyme.
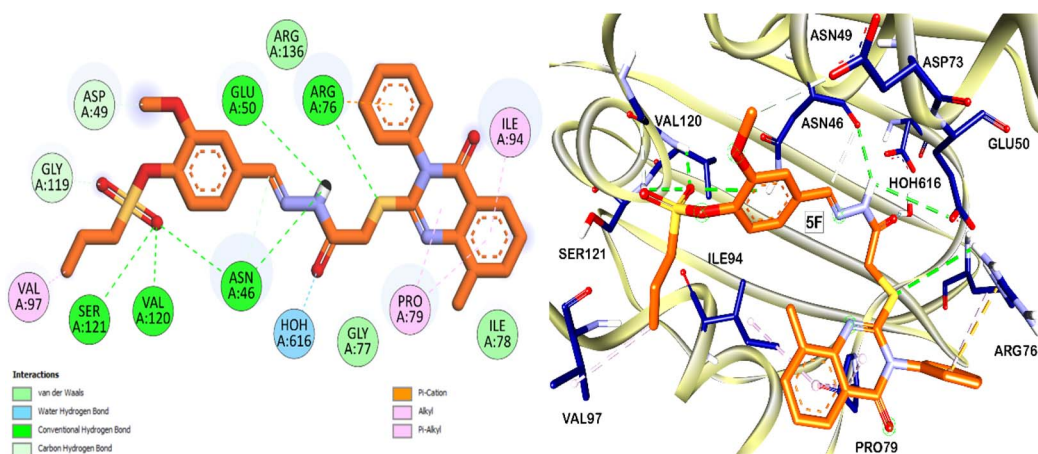

Fig. 4 Proposed binding interactions (3D and 2D) of compound **5f** in the DNA gyrase enzyme active site. It shows the interactions of compound **5f** with the DNA gyrase enzyme active site in both 3D and 2D formats. Carbon atoms of **5f** are highlighted in orange for clarity.
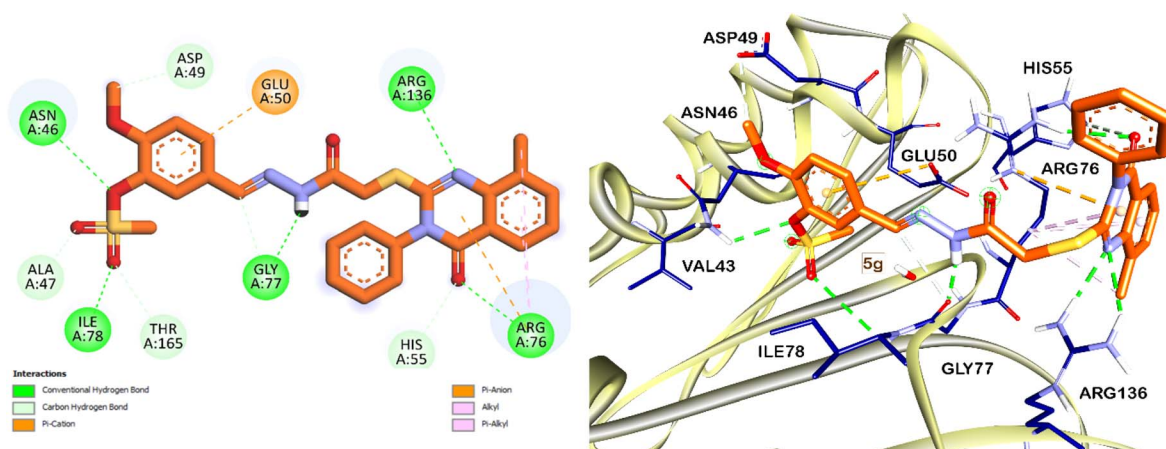

Fig. 5 Proposed binding interactions (3D and 2D) of compound **5g** in the DNA gyrase enzyme active site. It shows the interactions of compound **5g** with the DNA gyrase enzyme active site in both 3D and 2D formats. Carbon atoms of **5g** are highlighted in orange for clarity.

contribute to the antimicrobial activity of the quinazolinone derivatives, thereby providing valuable insights for future design and optimization of potent antimicrobial agents.

2.8. *In silico* pharmacokinetic analysis

The predicted pharmacokinetic characteristics and drug-like properties of the newly synthesized quinazolinone derivatives
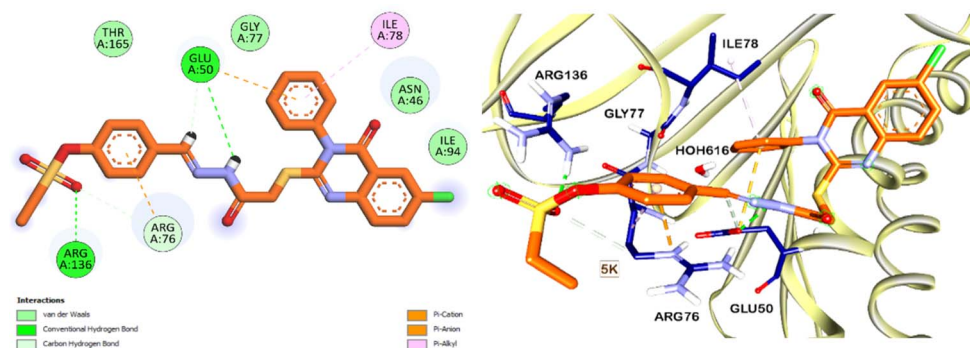
Fig. 6 Proposed binding interactions (3D and 2D) of compound **5k** in the DNA gyrase enzyme active site. It shows the interactions of compound **5k** with the DNA gyrase enzyme active site in both 3D and 2D formats. Carbon atoms of **5k** are highlighted in orange for clarity.

5a–r were assessed through the SwissADME server, emphasizing key pharmacokinetic considerations. These compounds exhibit metabolic stability and are not substrates for the various isoforms of CYP450 enzymes, which is significant for minimizing drug–drug interactions and enhancing metabolic predictability. Additionally, they are not substrates for P-glycoprotein (P-gp), indicating that they are likely to remain within cells and exert their therapeutic action without being effluxed by P-gp, which is a common resistance mechanism in many cancers and bacterial infections.

These derivatives display acceptable aqueous solubility, with a calculated topological polar surface area (TPSA) of approximately 150 Å², which is beneficial for their absorption and permeability. The compounds also exhibit suitable lipophilicity, with a consensus log P value around 4.1, suggesting a balanced hydrophilic–lipophilic profile that is crucial for bioavailability and cell membrane permeability (Table 4). Regarding Lipinski's rule of five, the compounds show only one violation: their molecular weight exceeds 500 daltons, averaging around 550 daltons. While this might typically raise concerns about

permeability and absorption, the other favorable properties mitigate this issue to some extent.

Moreover, these compounds demonstrate good synthetic accessibility, with an average score of 4 on the SwissADME scale, where 1 indicates an easy synthesis and 10 indicates a hard synthesis. This score reflects a moderate ease of synthesis, which is advantageous for further development and large-scale production. Overall, the quinazolinone derivatives exhibit promising pharmacokinetic properties. Future modifications could focus on reducing the molecular weight and enhancing aqueous solubility to optimize these compounds for further drug development. These adjustments could improve their pharmacodynamic profiles and therapeutic efficacy.

3. Materials and methods

The details about material and methods used in this study are provided in ESI file.†

Table 4 *In silico* assessment of pharmacokinetic parameters for compounds **5a–r**

No.	MW (g mol^{-1})	#H-bond acceptor	#H-bond donors	TPSA	Consensus log P	P-gp substrate	Synthetic accessibility	Lipinski #violations	Pains #alerts
5a	522.60	7	1	153.40	3.68	No	3.82	1	0
5b	536.62	8	1	156.89	4.51	No	4.08	1	0
5c	550.65	8	1	156.89	4.90	No	4.22	1	0
5d	580.68	9	1	166.12	4.94	No	4.36	1	0
5e	566.65	9	1	166.12	4.61	No	4.23	1	0
5f	580.68	9	1	166.12	4.94	No	4.36	1	0
5g	552.62	9	1	166.12	4.19	No	4.07	1	0
5h	566.65	9	1	166.12	4.57	No	4.22	1	0
5i	580.68	9	1	166.12	4.84	No	4.35	1	0
5j	543.01	8	1	156.89	4.41	No	3.79	1	0
5k	557.04	8	1	156.89	4.74	No	3.94	1	0
5l	571.07	8	1	156.89	5.18	No	4.07	2	0
5m	573.04	9	1	166.12	4.44	No	3.93	1	0
5n	587.07	9	1	166.12	4.79	No	4.08	1	0
5o	601.09	9	1	166.12	5.15	No	4.22	1	0
5p	573.04	9	1	166.12	4.41	No	3.92	1	0
5q	587.07	9	1	166.12	4.79	No	4.08	1	0
5r	601.09	9	1	166.12	5.13	No	4.21	1	0

3.1. Chemistry

3.1.1. General procedure for the synthesis of compounds 5a–r.
A mixture of quinazolinone derivatives 3a,b (1 mmol) and alkanesulfonyl aryl aldehydes 4a–i (1 mmol) was refluxed in EtOH (10 ml) containing a catalytic amount of glacial AcOH (1 ml) for 2 hrs. Upon cooling, the mixture poured onto ice/cold water, and the precipitate was collected, dried and recrystallized from EtOH to give 5a–r as colorless crystals.

3.1.1.1. 4-((2-(2-((8-Methyl-4-oxo-3-phenyl-3,4-dihydroquinazolin-2-yl)thio)acetyl)-hydrazono)methyl)phenyl methanesulfonate (5a). Yield: 84%; mp 250–252 °C; IR (KBr) cm^{-1}, v: 3320 (OH, tautomer), 3174 (NH), 1676 (C=O), 1618 (C=N), 1363 (SO$_2$), 1207 (C–O, C–N); ^{1}H NMR δ (ppm): 2.46 (s, 3H, CH$_3$), 3.42 (s, 3H, SO$_2$CH$_3$), 3.99 (s, 2H, CH$_2$, iminol tautomer), 4.51 (s, 2H, CH$_2$, amide tautomer), 7.34–7.37 (m, 1H, H-6′), 7.41–7.42 (d, 2H, J = 6.0 Hz, H-2″ and H-6″), 7.48 (brs, 2H, H-2 and H-6), 7.60 (brs, 3H, H-3″, H-4″ and H-5″), 7.65 (brs, 1H, H-7′), 7.81 (brs, 2H, H-3 and H-5), 7.90–7.92 (m, 1H, H-5′), 8.05 (s, 1H, CH=N, iminol tautomer), 8.24 (s, 1H, CH=N, amide tautomer), 11.76 (s, 1H, OH/NH tautomer), 11.80 (s, 1H, OH/NH, tautomer); ^{13}C NMR δ (ppm): 16.62 (CH$_3$), 34.86 (CH$_2$), 37.52 (SO$_2$CH$_3$), 122.63 (C-2 and C-6), 124.12 (C-4′a), 125.41 (C-5′), 128.29 (C-2″ and C-6″), 128.61 (C-4), 129.32 (C-3″ and C-5″), 129.46 (C-3 and C-5), 129.86 (C-4″), 133.21 (C-6′), 133.96 (C-1″), 135.08 (C-8′), 135.84 (C-7′), 141.77 (C-8′a), 145.53 (HC=N), 149.80 (C-1), 155.90 (C-2′), 160.87 (CO-quinazolinone), 168.57 (CONH); anal. calc. for C$_{25}$H$_{22}$N$_4$O$_5$S$_2$ (522.59) C, 57.46; H, 4.24; N, 10.72. Found: C, 57.31; H, 4.38; N, 10.64.

3.1.1.2. 4-((2-(2-((8-Methyl-4-oxo-3-phenyl-3,4-dihydroquinazolin-2-yl)thio)acetyl)-hydrazono)methyl)phenyl ethanesulfonate (5b). Yield: 87%; mp 229–321 °C; IR (KBr) cm^{-1}, v: 3317 (OH, tautomer), 3177 (NH), 1677 (C=O), 1619 (C=N), 1388 (SO$_2$), 1219 (C–O, C–N); ^{1}H NMR δ (ppm): 1.38 (t, 3H, J = 5.5 Hz, CH$_3$CH$_2$), 2.45 (s, 3H, CH$_3$), 3.56 (q, 2H, J = 4.5 Hz, CH$_3$CH$_2$), 3.99 (s, 2H, CH$_2$, iminol tautomer), 4.50 (s, 2H, CH$_2$, amide tautomer), 7.34 (t, 1H, J = 7.5 Hz, H-6′), 7.37–7.40 (m, 2H, H-2″ and H-6″), 7.47 (d, 2H, J = 6.0 Hz, H-2 and H-6), 7.59 (brs, 3H, H-3″, H-4″ and H-5″), 7.65 (d, 1H, J = 6.5 Hz, H-7′), 7.80 (d, 2H, J = 8.5 Hz, H-3 and H-5), 7.91 (d, 1H, J = 7.5 Hz, H-5′), 8.05 (s, 1H, C=N, iminol tautomer), 8.24 (s, 1H, CH=N, amide tautomer), 11.76 (s, 1H, OH/NH tautomer) 11.80 (s, 1H, OH/NH, tautomer); ^{13}C NMR δ (ppm): 8.01 (CH$_3$CH$_2$), 16.65 (CH$_3$), 34.88 (CH$_2$), 44.82 (CH$_3$CH$_2$), 119.25 (C-4′a), 122.53 (C-2 and C-6), 124.13 (C-5′), 125.43 (C-4), 128.31 (C-2″ and C-6″), 128.61 (C-4″), 129.33 (C-3″ and C-5″), 129.49 (C-3 and C-5), 133.13 (C-6′), 134.00 (C-1″), 135.10 (C-8′), 135.86 (C-7′), 141.82 (C-8′a), 145.55 (HC=N), 149.67 (C-1), 155.91 (C-2′), 160.91 (CO-quinazolinone), 168.60 (CONH); anal. calc. for C$_{26}$H$_{24}$N$_4$O$_5$S$_2$ (536.62): C, 58.19; H, 4.51; N, 10.44. Found: C, 58.22; H, 4.46; N, 10.28.

3.1.1.3. 4-((2-(2-((8-Methyl-4-oxo-3-phenyl-3,4-dihydroquinazolin-2-yl)thio)acetyl)-hydrazono)methyl)phenyl propane-1-sulfonate (5c). Yield: 84%; mp 231–233 °C; IR (KBr) cm^{-1}, v: 3315 (OH, tautomer), 3178 (NH), 1676 (C=O), 1619 (C=N), 1370 (SO$_2$), 1210 (C–O, C–N); ^{1}H NMR δ (ppm): 1.04 (t, 3H, J = 8.0 Hz, CH$_3$CH$_2$CH$_2$), 1.85 (sextet, 2H, J = 7.5 Hz, CH$_3$CH$_2$CH$_2$), 2.45 (s, 3H, CH$_3$), 3.54 (t, 2H, J = 8.0 Hz, CH$_3$CH$_2$CH$_2$), 3.99 (s, 2H, CH$_2$, iminol tautomer), 4.50 (s, 2H, CH$_2$, amide tautomer), 7.34 (t, 1H, J = 7.5 Hz, H-6′), 7.37–7.40 (m, 2H, H-2″ and H-6″), 7.47 (dd, 2H, J = 7.5, 1.5 Hz, H-2 and H-6), 7.59–7.60 (m, 3H, H-3″, H-4″ and H-5″), 7.65 (d, 1H, J = 7.0 Hz, H-7′), 7.80 (d, 2H, J = 7.5 Hz, H-3 and H-5), 7.91 (d, 1H, J = 8.0 Hz, H-5′), 8.05 (s, 1H, CH=N, iminol tautomer), 8.24 (s, 1H, CH=N, amide tautomer), 11.76 (s, 1H, OH/NH, tautomer), 11.80 (s, 1H, OH/NH, tautomer); ^{13}C NMR δ (ppm): 12.31 (CH$_3$CH$_2$CH$_2$), 16.64 (CH$_3$), 16.93 (CH$_3$CH$_2$CH$_2$), 34.88 (CH$_2$), 51.49 (CH$_3$CH$_2$CH$_2$), 119.25 (C-4′a), 122.53 (C-2 and C-6), 124.12 (C-5′), 125.41 (C-4), 128.29 (C-2″ and C-6″), 128.62 (C-4″), 129.32 (C-3″ and C-5″), 129.49 (C-3 and C-5), 133.10 (C-6′), 133.97 (C-1″), 135.08 (C-8′), 135.85 (C-7′), 141.80 (C-8′a), 145.52 (HC=N), 149.63 (C-1), 155.88 (C-2′), 160.88 (CO-quinazolinone), 168.58 (CONH); anal. calc. for C$_{27}$H$_{26}$N$_4$O$_5$S$_2$ (550.65): C, 58.89; H, 4.76; N, 10.17. Found: C, 58.74; H, 4.59; N, 10.29.

3.1.1.4. 2-Methoxy-4-((2-(2-((8-methyl-4-oxo-3-phenyl-3,4-dihydroquinazolin-2-yl)thio)-acetyl)hydrazono)methyl)phenyl methanesulfonate (5d). Yield: 80%; mp 242–244 °C; IR (KBr) cm^{-1}, v: 3321 (OH, tautomer), 3170 (NH), 1671 (C=O), 1630 (C=N), 1340 (SO$_2$), 1217 (C–O, C–N); ^{1}H NMR δ (ppm): 2.46 (s, 3H, CH$_3$), 3.38 (s, 3H, SO$_2$CH$_3$), 3.88 (s, 3H, OCH$_3$), 4.00 (s, 2H, CH$_2$, iminol tautomer), 4.50 (s, 2H, CH$_2$, amide tautomer), 7.32–7.37 (m, 3H, H-6′, H-2″ and H-6″), 7.48 (brs, 2H, H-3 and H-7′), 7.60 (brs, 3H, H-3″, H-4″ and H-5″), 7.64–7.66 (m, 2H, H-5 and H-6), 7.90–7.92 (m, 1H, H-5′), 8.02 (s, 1H, CH=N, iminol tautomer), 8.22 (s, 1H, CH=N, amide tautomer), 11.80 (s, 1H, OH/NH, tautomer); ^{13}C NMR δ (ppm): 16.71 (CH$_3$), 34.85 (CH$_2$), 38.43 (SO$_2$CH$_3$), 56.05 (OCH$_3$), 111.17 (C-3), 119.26 (C-4′a), 119.36 (C-6), 124.15 (C-5), 125.21 (C-5′), 125.45 (C-4), 129.34 (C-2″ and C-6″), 129.50 (C-3″ and C-5″), 129.90 (C-4″), 134.01 (C-6′), 134.24 (C-1″), 135.13 (C-8′), 135.87 (C-7′), 138.79 (C-8′a), 142.16 (C-1), 145.56 (HC=N), 151.72 (C-2), 155.91 (C-2′), 160.92 (CO-quinazolinone), 168.60 (CONH); anal. calc. for C$_{26}$H$_{24}$N$_4$O$_6$S$_2$ (552.62): C, 56.51; H, 4.38; N, 10.14. Found: C, 56.38; H, 4.20; N, 10.09.

3.1.1.5. 2-Methoxy-4-((2-(2-((8-methyl-4-oxo-3-phenyl-3,4-dihydroquinazolin-2-yl)thio)-acetyl)hydrazono)methyl)phenyl ethanesulfonate (5e). Yield: 85%; mp 216–218 °C; IR (KBr) cm^{-1}, v: 3322 (OH), 3172 (NH), 1675 (C=O), 1636 (C=N), 1359 (SO$_2$), 1219 (C–O, C–N); ^{1}H NMR δ (ppm): 1.39 (t, 3H, J = 6.0 Hz, CH$_2$CH$_3$), 2.45 (s, 3H, CH$_3$), 3.51 (q, 2H, J = 5.5 Hz, CH$_2$CH$_3$), 3.88 (s, 3H, OCH$_3$), 4.00 (s, 2H, CH$_2$, iminol tautomer), 4.50 (s, 2H, CH$_2$, amide tautomer), 7.33–7.34 (m, 3H, H-6′, H-2″ and H-6″), 7.47 (brs, 2H, H-3 and H-7′), 7.60 (brs, 3H, H-3″, H-4″ and H-5″), 7.64–7.66 (m, 2H, H-5 and H-6), 7.90–7.92 (m, 1H, H-5′), 8.02 (s, 1H, C=N, iminol tautomer), 8.22 (s, 1H, CH=N, amide tautomer), 11.79 (s, 1H, OH/NH, tautomer), 11.81 (s, 1H, OH/NH, tautomer); ^{13}C NMR δ (ppm): 8.00 (CH$_2$CH$_3$), 16.66 (CH$_3$), 34.85 (CH$_2$), 45.67 (CH$_2$CH$_3$), 56.01 (OCH$_3$), 111.08 (C-3), 119.24 (C-4′a), 119.30 (C-6), 124.12 (C-5), 124.13 (C-5′), 125.41 (C-4), 129.31 (C-2″ and C-6″), 129.45 (C-3″ and C-5″), 129.89 (C-4″), 134.06 (C-6′), 134.12 (C-1″), 135.08 (C-8′), 135.09 (C-7′), 138.68 (C-8′a), 142.09 (C-1), 145.52 (HC=N), 151.62 (C-2), 155.89 (C-2′), 160.87 (CO-quinazolinone), 167.32 (CONH); anal. calc. for C$_{27}$H$_{26}$N$_4$O$_6$S$_2$ (566.65): C, 57.23; H, 4.63; N, 9.89. Found: C, 57.11; H, 4.50; N, 9.72.

3.1.1.6. 2-Methoxy-4-((2-(2-((8-methyl-4-oxo-3-phenyl-3,4-dihydroquinazolin-2-yl)thio)-acetyl)hydrazono)methyl)phenyl propane-1-sulfonate (5f). Yield: 78.5%; mp 206–208 °C; IR (KBr) cm^{-1}, ν: 3311 (OH, tautomer), 3173 (NH), 1679 (C=O), 1620 (C=N), 1350 (SO$_2$), 1221 (C–O, C–N); ^{1}H NMR δ (ppm): 1.04 (t, 3H, J = 7.0 Hz, CH$_3$CH$_2$CH$_2$), 1.90 (sextet, 2H, J = 7.0 Hz, CH$_3$CH$_2$CH$_2$), 2.45 (s, 3H, CH$_3$), 3.49 (t, 2H, J = 7.0 Hz, CH$_3$-CH$_2$CH$_2$), 3.88 (s, 3H, OCH$_3$), 4.00 (s, 2H, CH$_2$, iminol tautomer), 4.50 (s, 2H, CH$_2$, amide tautomer), 7.31–7.35 (m, 3H, H-6′, H-2″ and H-6″), 7.47–7.48 (m, 2H, H-3 and H-7′), 7.60 (brs, 3H, H-3″, H-4″ and H-5″), 7.64–7.66 (m, 2H, H-5 and H-6), 7.91 (d, 1H, J = 8.0 Hz, H-6), 8.02 (s, 1H, CH=N, iminol tautomer), 8.22 (s, 1H, CH=N, amide tautomer), 11.79 (s, 1H, OH/NH, tautomer), 11.82 (s, 1H, OH/NH, tautomer); ^{13}C NMR δ (ppm): 12.37 (CH$_3$CH$_2$CH$_2$), 16.68 (CH$_3$), 17.01 (CH$_3$CH$_2$CH$_2$), 34.82 (CH$_2$), 52.42 (CH$_3$CH$_2$CH$_2$), 56.03 (OCH$_3$), 111.07 (C-3), 119.24 (C-4′a), 119.33 (C-6), 124.13 (C-5), 124.19 (C-5′), 125.42 (C-4), 129.32 (C-2″ and C-6″), 129.47 (C-3″ and C-5″), 129.87 (C-4″), 133.98 (C-6′), 134.09 (C-1″), 135.08 (C-8′), 135.85 (C-7′), 138.69 (C-8′a), 142.12 (C-1), 145.54 (HC=N), 151.65 (C-2), 155.89 (C-2′), 160.89 (CO-quinazolinone), 168.56 (CONH); anal. calc. for C$_{28}$H$_{28}$N$_4$O$_6$S$_2$ (580.67): C, 57.92; H, 4.86; N, 9.65. Found: C, 57.80; H, 4.71; N, 9.50.

3.1.1.7. 2-Methoxy-5-((2-(2-((8-methyl-4-oxo-3-phenyl-3,4-dihydroquinazolin-2-yl)thio)-acetyl)hydrazono)methyl)phenyl methanesulfonate (5g). Yield: 86%; mp 229–231 °C; IR (KBr) cm^{-1}, ν: 3316 (OH, tautomer), 3180 (NH), 1669 (C=O), 1628 (C=N), 1344 (SO$_2$), 1229 (C–O, C–N); ^{1}H NMR δ (ppm): 2.46 (s, 3H, CH$_3$), 3.38 (s, 3H, SO$_2$CH$_3$), 3.90 (s, 3H, OCH$_3$), 3.99 (s, 2H, CH$_2$, iminol tautomer), 4.50 (s, 2H, CH$_2$, amide tautomer), 7.25–7.29 (m, 1H, H-3), 7.33–7.36 (m, 1H, H-6′), 7.48 (d, 2H, J = 7.0 Hz, H-2″ and H-6″), 7.60 (d, 2H, J = 6.5 Hz, H-3″ and H-5″), 7.63–7.65 (m, 3H, H-4, H-7′ and H-4″), 7.90–7.92 (m, 2H, H-6 and H-5′), 7.99 (s, 1H, CH=N, iminol tautomer), 8.16 (s, 1H, CH=N, amide tautomer), 11.68 (s, 1H, OH/NH, tautomer), 11.71 (s, 1H, OH/NH, tautomer); ^{13}C NMR δ (ppm): 16.69 (CH$_3$), 35.01 (CH$_2$), 38.41 (SO$_2$CH$_3$), 56.21 (OCH$_3$), 113.67 (C-3), 119.25 (C-4′a), 121.47 (C-6), 121.74 (C-4), 124.11 (C-5′), 125.39 (C-6), 127.21 (C-5), 129.33 (C-2″ and C-6″), 129.47 (C-3″ and C-5″), 129.85 (C-4″), 134.05 (C-1″), 135.06 (C-8′), 135.88 (C-7′), 138.10 (C-8′a), 141.97 (C-1), 145.54 (HC=N), 152.65 (C-2), 155.94 (C-2′), 160.90 (CO-quinazolinone), 168.39 (CONH); anal. calc. for C$_{26}$H$_{24}$N$_4$O$_6$S$_2$ (552.62): C, 56.51; H, 4.38; N, 10.14. Found: C, 56.63; H, 4.51; N, 10.28.

3.1.1.8. 2-Methoxy-5-((2-(2-((8-methyl-4-oxo-3-phenyl-3,4-dihydroquinazolin-2-yl)thio)-acetyl)hydrazono)methyl)phenyl ethanesulfonate (5h). Yield: 80.5%; mp 234–236 °C; IR (KBr) cm^{-1}, ν: 3320 (OH, tautomer), 3165 (NH), 1677 (C=O), 1618 (C=N), 1350 (SO$_2$), 1211 (C–O, C–N); ^{1}H NMR δ (ppm): 1.39 (t, 3H, J = 7.0 Hz, CH$_2$CH$_3$), 2.46 (s, 3H, CH$_3$), 3.51 (q, 2H, J = 7.5 Hz, CH$_2$CH$_3$), 3.89 (s, 3H, OCH$_3$), 3.99 (s, 2H, CH$_2$, iminol tautomer), 4.50 (s, 2H, CH$_2$, amide tautomer), 7.25–7.28 (m, 1H, H-3), 7.33–7.36 (m, 1H, H-6′), 7.47 (brs, 2H, H-2″ and H-6″), 7.60 (brs, 2H, H-3″ and H-5″), 7.61–7.64 (m, 3H, H-4, H-7′ and H-4″), 7.91–7.92 (m, 2H, H-6 and H-5′), 7.99 (s, 1H, CH=N, iminol tautomer), 8.16 (s, 1H, CH=N, amide tautomer), 11.67 (s, 1H,

OH/NH, tautomer), 11.70 (s, 1H, OH/NH, tautomer); ^{13}C NMR δ (ppm): 8.02 (CH$_2$CH$_3$), 16.71 (CH$_3$), 34.97 (CH$_2$), 45.73 (CH$_2$CH$_3$), 56.22 (OCH$_3$), 113.63 (C-3), 119.27 (C-4′a), 121.42 (C-6), 121.59 (C-4), 124.13 (C-5′), 125.42 (C-6), 127.15 (C-5), 129.34 (C-2″ and C-6″), 129.49 (C-3″ and C-5″), 129.89 (C-4″), 134.08 (C-1″), 135.08 (C-8′), 135.88 (C-7′), 138.02 (C-8′a), 142.02 (C-1), 145.56 (HC=N), 152.61 (C-2), 155.95 (C-2′), 160.93 (CO-quinazolinone), 168.40 (CONH); anal. calc. for C$_{27}$H$_{26}$N$_4$O$_6$S$_2$ (566.65): C, 57.23; H, 4.63; N, 9.89. Found: C, 57.38; H, 4.51; N, 9.75.

3.1.1.9. 2-Methoxy-5-((2-(2-((8-methyl-4-oxo-3-phenyl-3,4-dihydroquinazolin-2-yl)thio)-acetyl)hydrazono)methyl)phenyl propane-1-sulfonate (5i). Yield: 90.5%; mp 256–258 °C; IR (KBr) cm^{-1}, ν: 3315 (OH, tautomer), 3172 (NH), 1673 (C=O), 1631 (C=N), 1349 (SO$_2$), 1221 (C–O, C–N); ^{1}H NMR δ (ppm): 1.03 (t, 3H, J = 7.0 Hz, CH$_3$CH$_2$CH$_2$), 1.88 (sextet, 2H, J = 7.0 Hz, CH$_3$CH$_2$CH$_2$), 2.46 (s, 3H, CH$_3$), 3.47 (t, 2H, J = 6.0 Hz, CH$_3$-CH$_2$CH$_2$), 3.89 (s, 3H, OCH$_3$), 3.99 (s, 2H, CH$_2$, iminol tautomer), 4.50 (s, 2H, CH$_2$, amide tautomer), 7.24–7.28 (m, 1H, H-3), 7.32–7.35 (m, 1H, H-6′), 7.48 (brs., 2H, H-2″ and H-6″), 7.60 (brs., 2H, H-3″ and H-5″), 7.61–7.64 (m, 3H, H-4, H-7′ and H-4″), 7.90–7.92 (m, 2H, H-6 and H-5′), 7.98 (s, 1H, CH=N, iminol tautomer), 8.17 (s, 1H, CH=N, amide tautomer), 11.68 (s, 1H, OH/NH, tautomer), 11.72 (s, 1H, OH/NH, tautomer); ^{13}C NMR δ (ppm): 12.37 (CH$_3$CH$_2$CH$_2$), 16.68 (CH$_3$), 17.01 (CH$_3$CH$_2$CH$_2$), 34.82 (CH$_2$), 52.42 (CH$_3$CH$_2$CH$_2$), 56.03 (OCH$_3$), 111.67 (C-3), 119.24 (C-4′a), 119.33 (C-6), 124.13 (C-4), 124.19 (C-5′), 125.42 (C-6), 129.32 (C-2″ and C-6″), 129.47 (C-3″ and C-5″), 129.87 (C-4″), 133.98 (C-5), 134.09 (C-1″), 135.08 (C-8′), 135.85 (C-7′), 138.69 (C-8′a), 142.12 (C-1), 145.54 (HC=N), 151.65 (C-2), 155.89 (C-2′), 160.89 (CO-quinazolinone), 168.56 (CONH); anal. calc. for C$_{28}$H$_{28}$N$_4$O$_6$S$_2$ (580.67): C, 57.92; H, 4.86; N, 9.65. Found: C, 57.82; H, 4.99; N, 9.51.

3.1.1.10. 4-((2-(2-((6-Chloro-4-oxo-3-phenyl-3,4-dihydroquinazolin-2-yl)thio)acetyl)-hydrazono)methyl)phenyl methanesulfonate (5j). Yield: 90%; mp 236–238 °C; IR (KBr) cm^{-1}, ν: 3325 (OH, tautomer), 3170 (NH), 1671 (C=O), 1620 (C=N), 1355 (SO$_2$), 1214 (C–O, C–N); ^{1}H NMR δ (ppm): 3.33 (s, 3H, SO$_2$CH$_3$), 3.98 (s, 2H, CH$_2$, iminol tautomer), 4.46 (s, 2H, CH$_2$, amide tautomer), 7.41 (brs, 1H, H-8′), 7.49 (brs, 2H, H-2″ and H-6″), 7.59 (brs, 2H, H-2 and H-6), 7.79–7.81 (m, 3H, H-3″, H-4″ and H-5″), 7.85–7.86 (m, 2H, H-3 and H-5), 7.98–8.00 (m, 2H, H-5′ and H-7′), 8.06 (s, 1H, CH=N, iminol tautomer), 8.28 (s, 1H, CH=N, amide tautomer), 11.71 (s, 1H, OH/NH, tautomer), 11.82 (s, 1H, OH/NH, tautomer); ^{13}C NMR δ (ppm): 34.26 (CH$_2$), 37.54 (SO$_2$CH$_3$), 120.77 (C-4′a), 122.70 (C-2 and C-6), 125.48 (C-4), 128.14 (C-5), 128.45 (C-2″ and C-6″), 128.72 (C-4″), 129.27 (C-3″ and C-5″), 129.56 (C-3 and C-5), 130.07 (C-8′), 133.17 (C-6′), 134.92 (C-1″), 135.55 (C-7′), 142.06 (C-8′a), 145.79 (HC=N), 149.85 (C-1), 157.84 (C-2′), 159.66 (CO-quinazolinone), 168.71 (CONH); C$_{24}$H$_{19}$ClN$_4$O$_5$S$_2$ (543.01): C, 53.09; H, 3.53; N, 10.32. Found: C, 53.18; H, 3.41; N, 10.21

3.1.1.11. 4-((2-(2-((6-Chloro-4-oxo-3-phenyl-3,4-dihydroquinazolin-2-yl)thio)acetyl)-hydrazono)methyl)phenyl ethanesulfonate (5k). Yield: 81%; mp 170–172 °C; IR (KBr) cm^{-1}, ν: 3321 (OH, tautomer), 3173 (NH), 1673 (C=O), 1622 (C=N), 1360 (SO$_2$), 1210 (C–O, C–N); ^{1}H NMR δ (ppm): 1.38 (t, 3H, J =

7.0 Hz, CH$_2$CH$_3$), 3.55 (q, 2H, J = 7.5 Hz, CH$_2$CH$_3$), 3.99 (s, 2H, CH$_2$, iminol tautomer), 4.46 (s, 2H, CH$_2$, amide tautomer), 7.38–7.39 (m, 1H, H-8′), 7.48–7.51 (m, 2H, H-2″ and H-6″), 7.58–7.61 (m, 2H, H-2 and H-6), 7.78–7.79 (m, 3H, H-3″, H-4″ and H-5″), 7.82–7.87 (m, 3H, J = 8.5, 1.5 Hz, H-3, H-5 and H-7′), 8.00 (s, 1H, H-5′), 8.06 (s, 1H, CH=N, iminol tautomer), 8.28 (s, 1H, CH=N, amide tautomer), 11.72 (s, 1H, OH/NH, tautomer), 11.83 (s, 1H, OH/NH, tautomer); ^{13}C NMR δ (ppm): 8.00 (CH$_2$CH$_3$), 34.27 (CH$_2$), 44.79 (CH$_2$CH$_3$), 120.74 (C-4′a), 122.54 (C-2 and C-6), 125.45 (C-4), 128.12 (C-5′), 128.41 (C-2″ and C-6″), 128.69 (C-4″), 129.24 (C-3″ and C-5″), 129.53 (C-3 and C-5), 130.03 (C-8′), 133.04 (C-6′), 134.88 (C-1″), 135.53 (C-7′), 142.05 (C-8′a), 145.75 (HC=N), 149.67 (C-1), 157.80 (C-2′), 159.66 (CO-quinazolinone), 168.66 (CONH); anal. calc. for C$_{25}$H$_{21}$ClN$_4$O$_5$S$_2$ (557.04): C, 53.91; H, 3.80; N, 10.06. Found: C, 53.85; H, 3.65; N, 10.19.

3.1.1.12. 4-((2-(2-((6-Chloro-4-oxo-3-phenyl-3,4-dihydroquinazolin-2-yl)thio)acetyl)-hydrazono)methyl)phenyl propane-1-sulfonate (5l). Yield: 82.5%; mp 179–181 °C; IR (KBr) cm^{-1}, ν: 3317 (OH, tautomer), 3168 (NH), 1679 (C=O), 1630 (C=N), 1360 (SO$_2$), 1210 (C–O, C–N); ^{1}H NMR δ (ppm): 1.04 (t, 3H, J = 7.5 Hz, CH$_3$CH$_2$CH$_2$), 1.86 (sextet, 2H, J = 7.5 Hz, CH$_3$CH$_2$CH$_2$), 3.54 (t, 2H, J = 7.5 Hz, CH$_3$CH$_2$CH$_2$), 3.98 (s, 2H, CH$_2$, iminol tautomer), 4.46 (s, 2H, CH$_2$, amide tautomer), 7.38 (d, 1H, J = 8.0 Hz, H-8′), 7.49–7.50 (m, 2H, H-2″ and H-6″), 7.59–7.61 (m, 2H, H-2 and H-6), 7.78–7.79 (m, 3H, H-3″, H-4″ and H-5″), 7.82–7.87 (m, 3H, H-3, H-5 and H-7′), 8.00 (s, 1H, H-5′), 8.06 (s, 1H, CH=N, iminol tautomer), 8.27 (s, 1H, CH=N, amide tautomer), 11.72 (s, 1H, OH/NH, tautomer), 11.83 (s, 1H, OH/NH, tautomer); ^{13}C NMR δ (ppm): 12.32 (CH$_3$CH$_2$CH$_2$), 16.94 (CH$_3$CH$_2$CH$_2$), 34.27 (CH$_2$), 51.49 (CH$_3$CH$_2$CH$_2$), 120.73 (C-4′a), 122.56 (C-2 and C-6), 125.45 (C-4), 128.11 (C-5′), 128.40 (C-2″ and C-6″), 128.69 (C-4″), 129.25 (C-3″ and C-5″), 129.53 (C-3 and C-5), 130.04 (C-8′), 133.02 (C-6′), 134.87 (C-1″), 135.53 (C-7′), 142.05 (C-8′a), 145.74 (HC=N), 149.66 (C-1), 157.80 (C-2′), 159.66 (CO-quinazolinone), 168.66 (CONH); anal. calc. for C$_{26}$H$_{23}$ClN$_4$O$_5$S$_2$ (571.06): C, 54.69; H, 4.06; N, 9.81. Found: C, 54.86; H, 4.17; N, 9.69.

3.1.1.13. 4-((2-(2-((6-Chloro-4-oxo-3-phenyl-3,4-dihydroquinazolin-2-yl)thio)acetyl)-hydrazono)methyl)-2-methoxyphenyl methanesulfonate (5m). Yield: 85.6%; mp 232–234 °C; IR (KBr) cm^{-1}, ν: 3327 (OH, tautomer), 3188 (NH), 1669 (C=O), 1623 (C=N), 1359 (SO$_2$), 1225 (C–O, C–N); ^{1}H NMR δ (ppm): 3.38 (s, 3H, SO$_2$CH$_3$), 3.89 (s, 3H, OCH$_3$), 3.99 (s, 2H, CH$_2$, iminol tautomer), 4.48 (s, 2H, CH$_2$, amide tautomer), 7.31–7.36 (m, 2H, H-6 and H-8′), 7.48–7.49 (m, 3H, H-5′, H-2″ and H-6″), 7.59–7.60 (m, 3H, H-3″, H-4″ and H-5″), 7.82 (d, 1H, J = 8.5 Hz, H-5), 7.85 (d, 1H, J = 8.5 Hz, H-7′), 8.00 (brs, 1H, H-3), 8.04 (s, 1H, CH=N, iminol tautomer). 8.26 (s, 1H, CH=N, amide tautomer), 11.78 (s, 1H, OH/NH, tautomer); ^{13}C NMR δ (ppm): 34.45 (CH$_2$), 38.41 (SO$_2$CH$_3$), 55.99 (OCH$_3$), 111.06 (C-3), 119.52 (C-4′a), 120.23 (C-6), 120.73 (C-5), 124.24 (C-5′), 125.49 (C-6′), 128.06 (C-4), 129.26 (C-2″ and C-6″), 129.55 (C-3″ and C-5″), 130.07 (C-4″), 134.19 (C-1″), 134.90 (C-8′), 135.54 (C-7′), 138.79 (C-1), 142.24 (C-8′a), 145.78 (HC=N), 151.68 (C-2), 157.84 (C-2′), 159.69 (CO-quinazolinone), 168.71 (CONH); anal. calc. for C$_{25}$H$_{21}$ClN$_4$O$_6$S$_2$ (573.04): C, 52.40; H, 3.69; N, 9.78. Found: C, 52.58; H, 3.59; N, 9.64.

3.1.1.14. 4-((2-(2-((6-Chloro-4-oxo-3-phenyl-3,4-dihydroquinazolin-2-yl)thio)acetyl)-hydrazono)methyl)-2-methoxyphenyl ethanesulfonate (5n). Yield: 78.5%; mp 210–212 °C; IR (KBr) cm^{-1}, ν: 3316 (OH, tautomer), 3185 (NH), 1670 (C=O), 1630 (C=N), 1349 (SO$_2$), 1207 (C–O, C–N); ^{1}H NMR δ (ppm): 1.39 (t, 3H, J = 5.5 Hz, CH$_2$CH$_3$), 3.50 (q, 2H, J = 6.5 Hz, CH$_2$CH$_3$), 3.88 (s, 3H, OCH$_3$), 3.99 (s, 2H, CH$_2$, iminol tautomer), 4.48 (s, 2H, CH$_2$, amide tautomer), 7.31–7.34 (m, 2H, H-6 and H-8′), 7.48 (brs, 3H, H-6, H-2″ and H-6″), 7.59 (brs, 3H, H-3″, H-4″ and H-5″), 7.82 (d, 1H, J = 8.5 Hz, H-5), 7.86 (d, 1H, J = 8.5 Hz, H-7′), 8.00 (s, 1H, H-3), 8.03 (s, 1H, CH=N, iminol tautomer). 8.26 (s, 1H, CH=N, amide tautomer), 11.77 (s, 1H, OH/NH, tautomer), 11.83 (s, 1H, OH/NH, tautomer); ^{13}C NMR δ (ppm): 8.02 (CH$_2$CH$_3$), 34.43 (CH$_2$), 45.70 (CH$_2$CH$_3$), 55.96 (OCH$_3$), 111.00 (C-3), 119.47 (C-4′a), 120.18 (C-6), 120.72 (C-5), 124.12 (C-5′), 125.46 (C-6′), 128.05 (C-4), 129.24 (C-2″ and C-6″), 129.93 (C-3″ and C-5″), 130.03 (C-4″), 134.03 (C-1″), 134.88 (C-8′), 135.53 (C-7′), 138.70 (C-1), 142.19 (C-8′a), 145.74 (HC=N), 151.61 (C-2), 157.82 (C-2′), 159.65 (CO-quinazolinone), 168.67 (CONH); anal. calc. for C$_{26}$H$_{23}$ClN$_4$O$_6$S$_2$ (587.06): C, 53.19; H, 3.95; N, 9.54. Found: C, 53.30; H, 3.80; N, 9.39.

3.1.1.15. 4-((2-(2-((6-Chloro-4-oxo-3-phenyl-3,4-dihydroquinazolin-2-yl)thio)acetyl)-hydrazono)methyl)-2-methoxyphenyl propane-1-sulfonate (5o). Yield: 82%; mp 206–208 °C; IR (KBr) cm^{-1}, ν: 3319 (OH, tautomer), 3189 (NH), 1682 (C=O), 1622 (C=N), 1360 (SO$_2$), 1219 (C–O, C–N); ^{1}H NMR δ (ppm): 1.04 (t, 3H, J = 7.0 Hz, CH$_3$CH$_2$CH$_2$), 1.87 (sextet, 2H, J = 7.0 Hz, CH$_3$CH$_2$CH$_2$), 3.48 (t, 2H, J = 7.5 Hz, CH$_3$CH$_2$CH$_2$), 3.88 (s, 3H, OCH$_3$), 3.99 (s, 2H, CH$_2$, iminol tautomer), 4.47 (s, 2H, CH$_2$, amide tautomer), 7.32–7.34 (m, 2H, H-6 and H-8′), 7.48–7.49 (m, 3H, H-5′, H-2″ and H-6″), 7.58–7.60 (m, 3H, H-3″, H-4″ and H-5″), 7.82 (dd, 1H, J = 8.5, 2.5 Hz, H-5), 7.86 (dd, 1H, J = 8.5, 2.5 Hz, H-7′), 8.00 (s, 1H, H-3), 8.03 (s, 1H, CH=N, iminol tautomer), 8.25 (s, 1H, CH=N, amide tautomer), 11.77 (s, 1H, OH/NH, tautomer), 11.82 (s, 1H, OH/NH, tautomer); ^{13}C NMR δ (ppm): 12.41 (CH$_3$CH$_2$CH$_2$), 17.05 (CH$_3$CH$_2$CH$_2$), 34.46 (CH$_2$), 52.46 (CH$_3$CH$_2$CH$_2$), 56.02 (OCH$_3$), 111.03 (C-3), 119.55 (C-4′a), 120.28 (C-6), 120.76 (C-5), 124.27 (C-5′), 125.50 (C-6′), 128.10 (C-4), 129.28 (C-2″ and C-6″), 129.58 (C-3″ and C-5″), 130.09 (C-4″), 134.08 (C-1″), 134.94 (C-8′), 135.56 (C-7′), 138.74 (C-1), 142.28 (C-8′a), 145.80 (HC=N), 151.66 (C-2), 157.86 (C-2′), 159.71 (CO-quinazolinone), 168.74 (CONH); anal. calc. for C$_{27}$H$_{25}$ClN$_4$O$_6$S$_2$ (601.09): C, 53.95; H, 4.19; N, 9.32. Found: C, 53.81; H, 4.10; N, 9.19.

3.1.1.16. 5-((2-(2-((6-Chloro-4-oxo-3-phenyl-3,4-dihydroquinazolin-2-yl)thio)acetyl)-hydrazono)methyl)-2-methoxyphenyl methanesulfonate (5p). Yield: 82%; mp 240–242 °C; IR (KBr) cm^{-1}, ν: 3310 (OH, tautomer), 3185 (NH), 1672 (C=O), 1636 (C=N), 1345 (SO$_2$), 1218 (C–O, C–N); ^{1}H NMR δ (ppm): 3.40 (s, 3H, SO$_2$CH$_3$), 3.90 (s, 3H, OCH$_3$), 3.98 (s, 2H, CH$_2$, iminol tautomer), 4.48 (s, 2H, CH$_2$, amide tautomer), 7.27 (brs, 1H, H-3), 7.49–7.53 (m, 3H, H-8′, H-2″ and H-6″), 7.59–7.61 (m, 4H, H-6, H-3″, H-4″ and H-5″), 7.66 (brs, 1H, H-5′), 7.80 (d, 1H, J = 7.5 Hz, H-4), 7.86 (d, 1H, J = 7.5 Hz, H-7′), 8.00 (s, 1H, CH=N, iminol tautomer), 8.20 (s, 1H, CH=N, amide tautomer), 11.66 (s, 1H, OH/NH, tautomer), 11.74 (s, 1H, OH/NH, tautomer); ^{13}C NMR δ (ppm): 34.60 (CH$_2$), 38.40 (SO$_2$CH$_3$), 56.21 (OCH$_3$),

113.67 (C-3), 120.75 (C-4′a), 121.36 (C-6), 125.43 (C-5), 127.16 (C-5′), 127.39 (C-6′), 127.50 (C-4), 128.15 (C-1″), 129.24 (C-2″ and C-6″), 129.51 (C-3″ and C-5″), 130.02 (C-4″), 134.81 (C-8′), 135.54 (C-7′), 138.09 (C-1), 142.05 (C-8′a), 145.77 (HC=N), 152.64 (C-2), 157.84 (C-2′), 159.67 (CO-quinazolinone), 168.48 (CONH); anal. calc. for $C_{25}H_{21}ClN_4O_6S_2$ (573.04): C, 52.40; H, 3.69; N, 9.78. Found: C, 52.58; H, 3.51; N, 9.69.

3.1.1.17. 5-((2-(2-((6-Chloro-4-oxo-3-phenyl-3,4-dihydroquinazolin-2-yl)thio)acetyl)-hydrazono)methyl)-2-methoxyphenyl ethanesulfonate (5q). Yield: 81%; mp 208–210 °C; IR (KBr) cm^{-1}, ν: 3314 (OH, tautomer), 3187 (NH), 1683 (C=O), 1624 (C=N), 1366 (SO$_2$), 1220 (C–O, C–N); ^{1}H NMR δ (ppm): 1.40 (t, 3H, J = 7.0 Hz, CH$_3$CH$_2$), 3.53 (q, 2H, J = 7.0 Hz, CH$_3$CH$_2$), 3.89 (s, 3H, OCH$_3$), 3.97 (s, 2H, CH$_2$, iminol tautomer), 4.47 (s, 2H, CH$_2$, amide tautomer), 7.24–7.27 (m, 1H, H-3), 7.49 (d, 2H, J = 7.5 Hz, H-2″ and H-6″), 7.53 (d, 1H, J = 8.5 Hz, H-8′), 7.59–7.62 (m, 4H, H6, H-3″, H-4″ and H-5″), 7.65 (d, 1H, J = 1.5 Hz, H-5′), 7.80 (dd, 1H, J = 9.0, 2.0 Hz, H-4), 7.86 (dd, 1H, J = 8.5, 2.0 Hz, H-7′), 8.00 (s, 1H, CH=N, iminol tautomer), 8.20 (s, 1H, CH=N, amide tautomer), 11.66 (s, 1H, OH/NH, tautomer), 11.73 (s, 1H, OH/NH, tautomer); ^{13}C NMR δ (ppm): 8.17 (CH$_3$), 34.82 (CH$_2$), 45.91 (CH$_2$CH$_3$), 56.38 (OCH$_3$), 113.76 (C-3), 120.83 (C-4′a), 121.41 (C-6), 121.76 (C-4), 125.60 (C-5′), 127.27 (C-6′), 127.58 (C-5), 127.79 (C-1″), 128.36 (C-8′), 129.37 (C-2″ and C-6″), 129.76 (C-3″ and C-5″), 130.29 (C-4″), 135.66 (C-7′), 138.14 (C-1), 142.43 (C-8′a), 145.93 (HC=N), 152.78 (C-2), 157.95 (C-2′), 159.92 (CO-quinazolinone), 168.75 (CONH); anal. calc. for $C_{26}H_{23}ClN_4O_6S_2$ (587.06): C, 53.19; H, 3.95; N, 9.54. Found: C, 53.25; H, 3.79; N, 9.69.

3.1.1.18. 5-((2-(2-((6-Chloro-4-oxo-3-phenyl-3,4-dihydroquinazolin-2-yl)thio)acetyl)-hydrazono)methyl)-2-methoxyphenyl propane-1-sulfonate (5r). Yield: 85%; mp 216–218 °C; IR (KBr) cm^{-1}, ν: 3311 (OH, tautomer), 3185 (NH), 1683 (C=O), 1637 (C=N), 1358 (SO$_2$), 1215 (C–O, C–N); ^{1}H NMR δ (ppm): 1.04 (t, 3H, J = 6.5 Hz, CH$_3$CH$_2$CH$_2$), 1.87 (sextet, 2H, J = 6.0 Hz, CH$_3$CH$_2$CH$_2$), 3.50 (t, 2H, J = 6.0 Hz, CH$_3$CH$_2$CH$_2$), 3.89 (s, 3H, OCH$_3$), 3.98 (s, 2H, CH$_2$, iminol tautomer), 4.47 (s, 2H, CH$_2$, amide tautomer), 7.25–7.28 (m, 1H, H-3), 7.49 (brs, 2H, H-2″ and H-6″), 7.53 (d, 1H, J = 8.5 Hz, H-8′), 7.56–7.64 (m, 4H, H-6, H-3″, H-4″ and H-5″), 7.65 (brs, 1H, H-5), 7.80 (d, 1H, J = 8.0, Hz, H-4), 7.86 (d, 1H, J = 8.5 Hz, H-7′), 8.00 (s, 1H, CH=N, iminol tautomer), 8.20 (s, 1H, CH=N, amide tautomer), 11.67 (s, 1H, OH/NH, tautomer), 11.71 (s, 1H, OH/NH, tautomer); ^{13}C NMR δ (ppm): 12.36 (CH$_3$CH$_2$CH$_2$), 17.02 (CH$_3$CH$_2$CH$_2$), 34.67 (CH$_2$), 52.39 (CH$_3$CH$_2$CH$_2$), 56.22 (OCH$_3$), 113.57 (C-3), 120.72 (C-4′a), 121.29 (C-6), 121.72 (C-4), 125.43 (C-5′), 127.13 (C-6′), 127.33 (C-5), 128.15 (C-1″), 129.24 (C-2″ and C-6″), 129.53 (C-3″ and C-5″), 130.03 (C-4″), 134.78 (C-8′), 135.60 (C-7′), 137.86 (C-1), 142.10 (C-8′a), 145.78 (HC=N), 152.60 (C-2), 157.86 (C-2′), 159.68 (CO-quinazolinone), 168.48 (CONH); anal. calc. for $C_{27}H_{25}ClN_4O_6S_2$ (601.09): C, 53.95; H, 4.19; N, 9.32. Found: C, 53.88; H, 4.31; N, 9.49.

3.2. Investigation of the antimicrobial susceptibility of the synthesized compounds

The efficiency of the prepared molecules to serve as bactericidal and fungicidal was evaluated following the standard procedure.[44–48] More details about the experiment used were provided in the ESI file†.

The study was approved by the Medical Research Ethical Committee of the National Research Centre (04461123).

3.3. Effect of the targeted synthesized compounds on the bacterial lipid peroxidation (LPO)

Oxidative stress on the bacterial cells was usually indicated by the oxidation of the fatty acid contents in the bacterial cell membrane.[49] Additional information is provided in the supplemental data.

3.4. Biofilm inhibition activity of the synthesized molecules

The compounds being inhibit the biofilm formation were also determined by the crystal violet method.[50] More details about the procedure are provided in the supplemental data.

3.5. Confocal laser scanning microscope

The effect of the most potent compounds against microbial pathogens was analyzed by confocal laser scanning microscopy (Leica Microsystems DMi8, GmbH, Wetzlar, Germany). Following the standard process.[51,52] More details about the procedure are provided in the supplemental data.

3.6. Docking studies on DNA gyrase enzyme

We conducted a molecular docking investigation to assess how a series of newly synthesized quinazolinone derivatives (5a–r) interact with the DNA gyrase enzyme (PDB code: 6F86). These synthesized compounds' binding interactions and affinities towards the DNA gyrase enzyme were analyzed. The study commenced by retrieving the X-ray crystal structure of the DNA gyrase enzyme from the Protein Data Bank (https://www.rcsb.org) using the specified PDB code (6F86). To prepare the receptor for docking simulations, Biovia Discovery Studio was employed to streamline the enzyme structure by removing redundant chains and water molecules. This process included the addition of polar hydrogens and the adjustment of partial charges. Subsequently, docking studies were performed using Autodock 4.2 software, with a detailed protocol provided in the supplemental data. The grid box used for docking was set to dimensions of 60 × 60 × 60 points with a grid spacing of 0.375 Å. The box was centered on the coordinates of the native ligand (CWW) in the crystal structure to ensure that the entire binding pocket was encompassed. The center of the grid was positioned at X: 61.8154, Y: 28.8269, and Z: 63.8559 Å. This setup ensures the grid adequately covers the active site for accurate docking predictions. For each docking run, 100 poses were generated using the Lamarckian Genetic Algorithm in AutoDock 4.2. These poses were ranked based on their binding free energy, and the lowest-energy pose was selected as the most likely binding conformation.

4. Conclusion

In conclusion, the present study describes the development of a novel series of quinazolinone–alkanesulfonate derivatives (5a–r) *via* the attachment of aryl alkanesulfonates to the quinazolinone core through thioacetohydrazide azomethine linkers. The antimicrobial evaluation of these newly synthesized compounds revealed reasonable bactericidal activities compared to standard drugs. Notably, derivatives 5g and 5k exhibited the greatest minimum inhibitory concentration (MIC) values against *Candida albicans*, while 5g was the most effective against *Staphylococcus aureus* with MIC = 12.5 μg mL^{-1}, which is half the value recorded for the standard drug Sulfadiazine. Furthermore, 5k significantly prevented biofilm formation for all tested bacterial pathogens, surpassing the performance of the standard drug Ciprofloxacin. Additionally, 5k caused elevated lipid peroxidation (LPO) when added to the tested microbial pathogens, and confocal laser scanning microscopy (CLSM) visualization revealed fewer live cells after treatment. The molecular docking studies against the DNA gyrase enzyme revealed strong binding interactions, particularly with the acid hydrazide core, which effectively interacted with key residues GLU50, ASN46, GLY77, and ASP136. These interactions highlight the core's critical role in binding affinity and align well with the observed antimicrobial efficacy of the compounds, suggesting their potential as effective antimicrobials.

5 Limitation of the study

It is important to interpret the findings of this study with caution. Specifically, assessments for genotoxicity, mutagenicity, developmental toxicity, reproductive toxicity, neurotoxicity, and immunotoxicity must be conducted before considering the results for further studies, including *in vivo*, preclinical, or clinical applications. These additional assessments will ensure the reliability and applicability of the findings in real-world scenarios, thereby enhancing the validity of subsequent research and potential therapeutic use.

Data availability

The authors declare that the data supporting the findings of this study are available within the paper. Should any raw data files be needed in another format they are available from the corresponding author upon a reasonable request.

Conflicts of interest

There are no conflicts to declare.

Acknowledgements

References

1 E. Toner, A. Adalja, G. K. Gronvall, A. Cicero and T. V. Inglesby, Antimicrobial resistance is a global health emergency, *Health Secur.*, 2015, **13**, 153–155, DOI: **10.1089/hs.2014.0088**.

2 G. Mancuso, A. Midiri, E. Gerace and C. Biondo, Bacterial Antibiotic Resistance: The Most Critical Pathogens, *Pathogens*, 2021, **10**, 1310, DOI: **10.3390/pathogens10101310**.

3 J. Scheres and K. Kuszewski, Ten Threats to Global Health in 2018 and 2019. A welcome and informative communication of WHO to everybody, Zeszyty Naukowe Ochrony Zdrowia, *Zdrowie Publiczne i Zarzadzanie*, 2019, **17**, 2–8.

4 S. K. Ahmed, S. Hussein, K. Qurbani, R. H. Ibrahim, A. Fareeq, K. A. Mahmood and M. G. Mohamed, Antimicrobial resistance: Impacts, challenges, and future prospects, *J. Med. Surg. Public Health*, 2024, **2**, 100081–100089, DOI: **10.1016/j.glmedi.2024.100081**.

5 M. A. Salam, M. Y. Al-Amin, M. T. Salam, J. S. Pawar, N. Akhter, A. A. Rabaan and M. A. A. Alqumber, Antimicrobial Resistance: A Growing Serious Threat for Global Public Health, *Healthcare*, 2023, **11**(13), 1946–1966, DOI: **10.3390/healthcare11131946**.

6 A. M. Almansour, M. A. Alhadlaq, K. O. Alzahrani, L. E. Mukhtar, A. L. Alharbi and S. M. Alajel, The Silent Threat: Antimicrobial-Resistant Pathogens in Food-Producing Animals and Their Impact on Public Health, *Microorganisms*, 2023, **11**(9), 2127, DOI: **10.3390/microorganisms11092127**.

7 C. Miranda, V. Silva, R. Capita, C. Alonso-Calleja, G. Igrejas and P. Poeta, Implications of antibiotics use during the COVID-19 pandemic: present and future, *J. Antimicrob. Chemother.*, 2020, **75**, 3413–3416, DOI: **10.1093/jac/dkaa350**.

8 R. Nieuwlaat, L. Mbuagbaw, D. Mertz, L. L. Burrows, D. M. Bowdish, L. Moja, G. D. Wright and H. J. Schünemann, Coronavirus disease 2019 and antimicrobial resistance: parallel and interacting health emergencies, *Clin. Infect. Dis.*, 2021, **72**, 1657–1659, DOI: **10.1093/cid/ciaa773**.

9 M. Bassetti and D. R. Giacobbe, A look at the clinical, economic, and societal impact of antimicrobial resistance in 2020, *Expert Opin. Pharmacother.*, 2020, **21**, 2067–2071, DOI: **10.1080/14656566.2020.1802427**.

10 L. Toro-Alzate, K. Hofstraat and D. H. de Vries, The pandemic beyond the pandemic: a scoping review on the social relationships between COVID-19 and antimicrobial resistance, *Int. J. Environ. Res. Public Health*, 2021, **18**, 8766, DOI: **10.3390/ijerph18168766**.

11 M. S. Mulani, E. E. Kamble, S. N. Kumkar, M. S. Tawre and K. R. Pardesi, Emerging Strategies to Combat ESKAPE Pathogens in the Era of Antimicrobial Resistance: A Review, *Front. Microbiol.*, 2019, **10**, 539, DOI: **10.3389/fmicb.2019.00539**.

12 G. M. Rossolini, F. Arena, P. Pecile and S. Pollini, Update on the antibiotic resistance crisis, *Curr. Opin. Pharmacol.*, 2014, **18**, 56, DOI: **10.1016/j.coph.2014.09.006**.

13 R. J. Fair and Y. Tor, Antibiotics and bacterial resistance in the 21st century, *Perspect. Medicin. Chem.*, 2014, **6**, DOI: **10.4137/PMC.S14459** PMC. S14459, doi:.

14 A. M. Borcea, I. Ionuț, O. Crișan and O. Oniga, An overview of the synthesis and antimicrobial, antiprotozoal, and antitumor activity of thiazole and bisthiazole derivatives, *Molecules*, 2021, **26**, 624, DOI: **10.3390/molecules26030624**.

15 M. Miethke, M. Pieroni, T. Weber, M. Brönstrup, P. Hammann, L. Halby, P. B. Arimondo, P. Glaser, B. Aigle and H. B. Bode, Towards the sustainable discovery and development of new antibiotics, *Nat. Rev. Chem.*, 2021, **5**, 726–749, DOI: **10.1038/s41570021003131**.

16 B. Liu, D. Jiang and G. Hu, The antibacterial activity of isatin hybrids, *Curr. Top. Med. Chem.*, 2022, **22**, 25–40, DOI: **10.2174/1568026621666211116090456**.

17 S. Kumar, S. M. Lim, K. Ramasamy, V. Mani, S. A. A. Shah and B. Narasimhan, Design, synthesis, antimicrobial and cytotoxicity study on human colorectal carcinoma cell line of new 4,4-(1,4-phenylene) bis (pyrimidin-2-amine) derivatives, *Chem. Cent. J.*, 2018, **12**, 1–13, DOI: **10.1186/s1306501804403**.

18 A. M. Alsibaee, H. M. Al-Yousef and H. S. Al-Salem, Quinazolinones, the Winning Horse in Drug Discovery, *Molecules*, 2023, **28**(3), 978, DOI: **10.3390/molecules28030978**.

19 A. M. Srour, D. H. Dawood and D. O. Saleh, Synthesis, 3D-pharmacophore modelling and 2D-QSAR study of new pyridine-3-carbonitriles as vasorelaxant active agents, *New J. Chem.*, 2021, **45**, 7731–7740, DOI: **10.1039/D0NJ06319C**.

20 A. A. Radwan, F. K. Alanazi, *Biological Activity of Quinazolinones. Quinazolinone and Quinazoline Derivatives*, IntechOpen, 2019, DOI: **10.5772/intechopen.90621**.

21 I. Khan, S. Zaib, S. Batool, N. Abbas, Z. Ashraf, J. Iqbal and A. Saeed, Quinazolines and quinazolinones as ubiquitous structural fragments in medicinal chemistry: An update on the development of synthetic methods and pharmacological diversification, *Bioorg. Med. Chem.*, 2016, **24**(11), 2361–2381, DOI: **10.1016/j.bmc.2016.03.031**.

22 A. Urbina, R. Lira, G. Visbal and J. Bartrolí, In vitro antiproliferative effects and mechanism of action of the new triazole derivative UR-9825 against the protozoan parasite trypanosoma (Schizotrypanum) cruzi, *Antimicrob. Agents Chemother.*, 2000, **44**(9), 2498–2502, DOI: **10.1128/aac.44.9.2498-2502.2000**.

23 S. J. Marcroft and T. D. Potter, The fungicide fluquinconazole applied as a seed dressing to canola reduces Leptosphaeria maculans (blackleg) severity in south-eastern Australia. Australas, *Plant Pathol.*, 2008, **37**, 396–401, DOI: **10.1071/AP08016**.

24 S. Gatadi, T. V. Lakshmi and S. Nanduri, 4(3H)-Quinazolinone derivatives: Promising antibacterial drug leads, *Eur. J. Med. Chem.*, 2019, **15**, 157–172, DOI: **10.1016/j.ejmech.2019.03.018**.

25 S. Rollas and S. G. Küçükgüzel, Biological Activities of Hydrazone Derivatives, *Molecules*, 2007, **12**, 1910–1939, DOI: **10.3390/12081910**.

26 M. A. Omar, R. A. El-Shiekh, D. H. Dawood, A. Temirak and A. M. Srour, HydrazoneSulfonate Hybrids as Potential Cholinesterase Inhibitors: Design, Synthesis and Molecular Modelling Simulation, Fut, *Med. Chem.*, 2023, **15**(24), 2269–2287, DOI: **10.4155/fmc-2023-0238**.

27 S. G. Komurc, S. Rollas, M. Ulgen, J. W. Gorrod and A. Çevikbas, Evaluation of some arylhydrazones of p-aminobenzoic acid hydrazide as antimicrobial agents and their *in vitro* hepatic microsomal metabolism, *Boll. Chim. Farm.*, 1995, **134**, 375–379 PMID: 7546542.

28 M. Ulgen, B. B. Durgun, S. Rollas and J. W. Gorrod, The *in vitro* hepatic microsomal metabolism of benzoic acic benzylidenehydrazide, *Drug Metab. Drug Interact.*, 1997, **13**, 285–294, DOI: **10.1515/DMDI.1997.13.4.285**.

29 L. Popiołek, Hydrazide–hydrazones as potential antimicrobial agents: overview of the literature since 2010, *Med. Chem. Res.*, 2017, **26**, 287–301, DOI: **10.1007/s00044-016-1756-y**.

30 S. Chen, Y. Zhang, Y. Liu and Q. Wang, Design, synthesis, acaricidal activities, and structure-activity relationship studies of novel oxazolines containing sulfonate moieties, *J. Agric. Food Chem.*, 2019, **11** **67**(49), 13544–13549, DOI: **10.1021/acs.jafc.9b05547**.

31 E. H. Glass, *Current Status of Pesticide Resistance in Insects and Mites Attacking Deciduous Orchard Crops, Research Progress on Insect Resistance*, Chapter 5, 1974, DOI: **10.4182/ECEM7264.II-1.17**.

32 S. Ramalingam, S. Periandy, S. Sugunakala, T. Prabhu and M. Bououdina, Insilico molecular modeling, docking and spectroscopic [FT-IR/FT-Raman/UV/NMR] analysis of Chlorfenson using computational calculations, *Spectrochim Acta A Mol. Biomol. Spectrosc.*, 2013, **115**, 118–135, DOI: **10.1016/j.saa.2013.06.034**.

33 R. Patel and T. P. Busulfan, [Updated 2022 Oct 17], n. *StatPearls [Internet]*, Treasure Island (FL), StatPearls Publishing, 2024 Jan-. Available from: **https://www.ncbi.nlm.nih.gov/books/NBK555986/**.

34 I. V. Nechepurenko, E. D. Shirokova, M. V. Khvostov, T. S. Frolova, O. I. Sinitsyna and A. M. Maksimov, Synthesis, hypolipidemic and antifungal activity of tetrahydroberberrubine sulfonates, *Russ. Chem. Bull.*, 2019, **68**, 1052–1060, DOI: **10.1007/s11172-019-2519-y**.

35 S. S. Ragab, A. M. Sweed and A. Srour, Synthesis and antiproliferative properties of schiff base hydrazones based on a spirocyclic pyrimidine, *Chemistryselect*, 2024, e202400161, DOI: **10.1002/slct.202400161**.

36 E. A. Kazancioğlu, M. Güney, M. Şentürk and C. T. Supuran, Simple methanesulfonates are hydrolyzed by the sulfatase carbonic anhydrase activity, *J. Enzyme Inhib. Med. Chem.*, 2012, **27**(6), 880–885, DOI: **10.3109/14756366.2011.637202**.

37 S. Gatadi, T. V. Lakshmi and S. Nanduri, 4(3H)-Quinazolinone derivatives: Promising antibacterial drug leads, *Eur. J. Med. Chem.*, 2019, **170**, 157–172, DOI: **10.1016/j.ejmech.2019.03.018**.

38 D. Murugesan, P. C. Ray, T. Bayliss, et al., 2-Mercapto-Quinazolinones as Inhibitors of Type II NADH Dehydrogenase and Mycobacterium tuberculosis:

Structure-Activity Relationships, Mechanism of Action and Absorption, Distribution, Metabolism, and Excretion Characterization, *ACS Infect Dis*, 2018, **4**(6), 954–969, DOI: **10.1021/acsinfecdis.7b00275**.

39 F. M. Sroor, A. F. El-Sayed and M. Abdelraof, Design, synthesis, structure elucidation, antimicrobial, molecular docking, and SAR studies of novel urea derivatives bearing tricyclic aromatic hydrocarbon rings, *Arch. Pharm.*, 2024, e2300738, DOI: **10.1002/ardp.202300738**.

40 H. T. Abdel-Mohsen, M. A. Omar, O. Kutkat, A. M. ElKerdawy, A. A. Osman, M. GabAllah, A. Mostafab, M. A. Ali and H. I. ElDiwani, Discovery of novel thioquinazoline-*N*-aryl-acetamide/*N*-arylacetohydrazide hybrids as anti-SARS-CoV-2 agents: Synthesis, *in vitro* biological evaluation, and molecular docking studies, *J. Mol. Struct.*, 2023, **1276**, 134690–134706, DOI: **10.1016/j.molstruc.2022.134690**.

41 S. Narramore, C. E. M. Stevenson, A. Maxwell, D. M. Lawson and C. W. G. Fishwick, New insights into the binding mode of pyridine-3-carboxamide inhibitors of E. coli DNA gyrase, *Bioorg. Med. Chem.*, 2019, **27**(16), 3546–3550, DOI: **10.1016/j.bmc.2019.06.015**.

42 BIOVIA, *Dassault Systèmes, [BIOVIA Discovery Studio Visualizer]*, [2021], San Diego: Dassault Systèmes, [2023].

43 G. M. Morris, R. Huey, W. Lindstrom, M. F. Sanner, R. K. BelewK, D. S. Goodsell and A. J. Olson, AutoDock4 and AutoDockTools4: Automated docking with selective receptor flexibility, *J. Comput. Chem.*, 2009, **30**(16), 2785–2791, DOI: **10.1002/jcc.21256**.

44 S. S. Ragab, A. M. Sweed, Z. K. Hamza, E. Shaban and A. A. El-Sayed, Design, synthesis, and antibacterial activity of spiropyrimidinone derivatives incorporated azo sulfonamide chromophore for polyester printing application, *Fibers Polym.*, 2022, **23**, 2114–2122, DOI: **10.1007/s12221-022-4032-4**.

45 S. S. Ragab, M. Abdelraof, A. A. Elrashedy and A. M. Sweed, Design, synthesis, molecular dynamic simulation studies, and antibacterial evaluation of new spirocyclic aminopyrimidines, *J. Mol. Struct.*, 2023, **1278**, 134912, DOI: **10.1016/j.molstruc.2023.134912**.

46 S. S. Ragab, N. E. Ibrahim, M. S. Abdel-Aziz, A. A. Elrashedy and A. K. Allayeh, Synthesis, biological activity, and molecular dynamic studies of new triazolopyrimidine derivatives, *Results Chem.*, 2023, **6**, 101163, DOI: **10.1016/j.rechem.2023.101163**.

47 M. Mahran, N. A. Hassan, D. A. A. Osman, S. S. Ragab and A. A. Hassan, Synthesis and biological evaluation of novel pyrimidines derived from 6-aryl-5-cyano-2-thiouracil, *Z. Naturforsch. C. J. Biosci.*, 2016, **71**(5–6), 133–140, DOI: **10.1515/znc-2015-0265**.

48 A. Sabt, M. T. Abdelrahman, M. Abdelraof and H. R. M. Rashdan, Investigation of novel mucorales fungal inhibitors: synthesis, In-silico study and anti-fungal potency of novel class of coumarin-6-sulfonamides-thiazole and thiadiazole hybrids, *ChemistrySelect*, 2022, **7**(17), e202200691, DOI: **10.1002/slct.202200691**.

49 S. X. T. Lianga, L. S. Wongb, Y. M. Limc, P. F. Leed and S. Djearamanea, Effects of Zinc Oxide nanoparticles on Streptococcus pyogenes, *S. Afr. J. Chem. Eng.*, 2020, **34**, 63–71, DOI: **10.1016/j.sajce.2020.05.009**.

50 M. Abdelraof, M. S. Hasanin, M. M. Farag and H. Y. Ahmed, Green synthesis of bacterial cellulose/bioactive glass nanocomposites: Effect of glass nanoparticles on cellulose yield, biocompatibility and antimicrobial activity, *Int. J. Biol. Macromol.*, 2019, **138**, 975–985, DOI: **10.1016/j.ijbiomac.2019.07.144**.

51 M. A. El-Bendary, M. Abdelraof, M. E. Moharam, E. M. Elmahdy and M. A. Allam, Potential of silver nanoparticles synthesized using low active mosquitocidal Lysinibacillus sphaericus as novel antimicrobial agents, *Prep. Biochem. Biotech.*, 2021, **51**(9), 925–935, DOI: **10.1080/10826068.2021.1875236**.

52 M. M. Qader, A. A. Hamed, S. Soldatou, M. Abdelraof, M. E. Elawady, A. S. I. Hassane, L. Belbahri, R. Ebel and M. E. Rateb, Antimicrobial and antibiofilm activities of the fungal metabolites isolated from the marine Endophytes Epicoccum nigrum M13 and Alternaria alternata 13A, *Mar. Drugs.*, 2021, **19**(4), 323, DOI: **10.3390/md19040232**.